Summer 6-19-2019

Delivering Signal-Altering Bacterial Effector Proteins to Mammalian Cells Using Cell-Penetrating Peptide Technology

Robert Dickson

Kennesaw State University

Thesis Dissertation

Delivering Signal-Altering Bacterial Effector Proteins to Mammalian Cells Using Cell-Penetrating Peptide Technology

---

Author: Robert Luke Dickson

Principle Investigator: Dr. Jonathan McMurry

Committee Members: Dr. Jonathan McMurry, Dr. Carol Chrestensen, Dr. Scott Nowak

Funded by: Kennesaw State University and the Georgia Research Alliance

TABLE OF CONTENTS

LIST OF FIGURES

ABSTRACT

A major role of the mitogen activated protein kinase (MAPK) pathway in eukaryotes is to activate the bacterial pathogen defense response upon the detection of bacterial products in the environment. This defensive signaling results in the induction of inflammation, the transcription of antimicrobial peptides, the modulation of the cell cycle and cell survival. Some Gram-negative bacteria have evolved needle-like structures called Type III Secretion Systems (T3SS) that secrete signal-altering molecules into the host cell to interrupt signaling pathways that would otherwise lead to the elimination of the bacterial infection. These signal-altering molecules are known as bacterial effector proteins (BEPs). Bacterial effectors YopJ and VopA have been shown to interfere with specific signaling molecules in the MAPK pathway; effectively inducing apoptosis in mammalian intestinal endothelial cells. In this study, we deliver these proteins to colon cancer cells to artificially induce cell death, using a novel cell-penetrating peptide (CPP) delivery system called TAT-CaM. Here, we show that the TAT-CaM system is capable of delivering YopJ into mammalian cells and that YopJ is capable of inducing cell death once delivered. Although we encountered issues with reproducibility, we believe that TAT-CaM-YopJ could be effective in inducing cell death in cancer cells in a reproducible manner after experimental adjustments.

1. INTRODUCTION

Under normal conditions, bacterial infection of eukaryotic tissues results in the induction of an immune response that leads to the elimination of the bacteria. Bacterial byproducts are detected by transmembrane pattern recognition receptors (PRRs) on the cell surface. After recognizing bacterial byproducts, these receptors activate signaling cascades that result in the transcription of antimicrobial and proinflammatory genes that work together to rid the tissue of infection. However, certain species of Gram-negative bacteria have developed specialized apparatus called Type III Secretion Systems (T3SS) to overcome this defensive mechanism. These needle-like structures are used to secrete various signal-altering molecules, known as bacterial effector proteins (BEPs), into the cells of the host tissue to interrupt signaling pathways, such as the mitogen-activated protein kinase (MAPK) pathway [1, 2, 3]. Interrupting these pathways shuts down transcription of defensive genes that would otherwise lead to the elimination of the infection [1, 2, 3]. Thus, T3SSs and bacterial effector proteins are adaptations that arose to allow bacteria to evade the host-cell immune response [1, 2, 3].

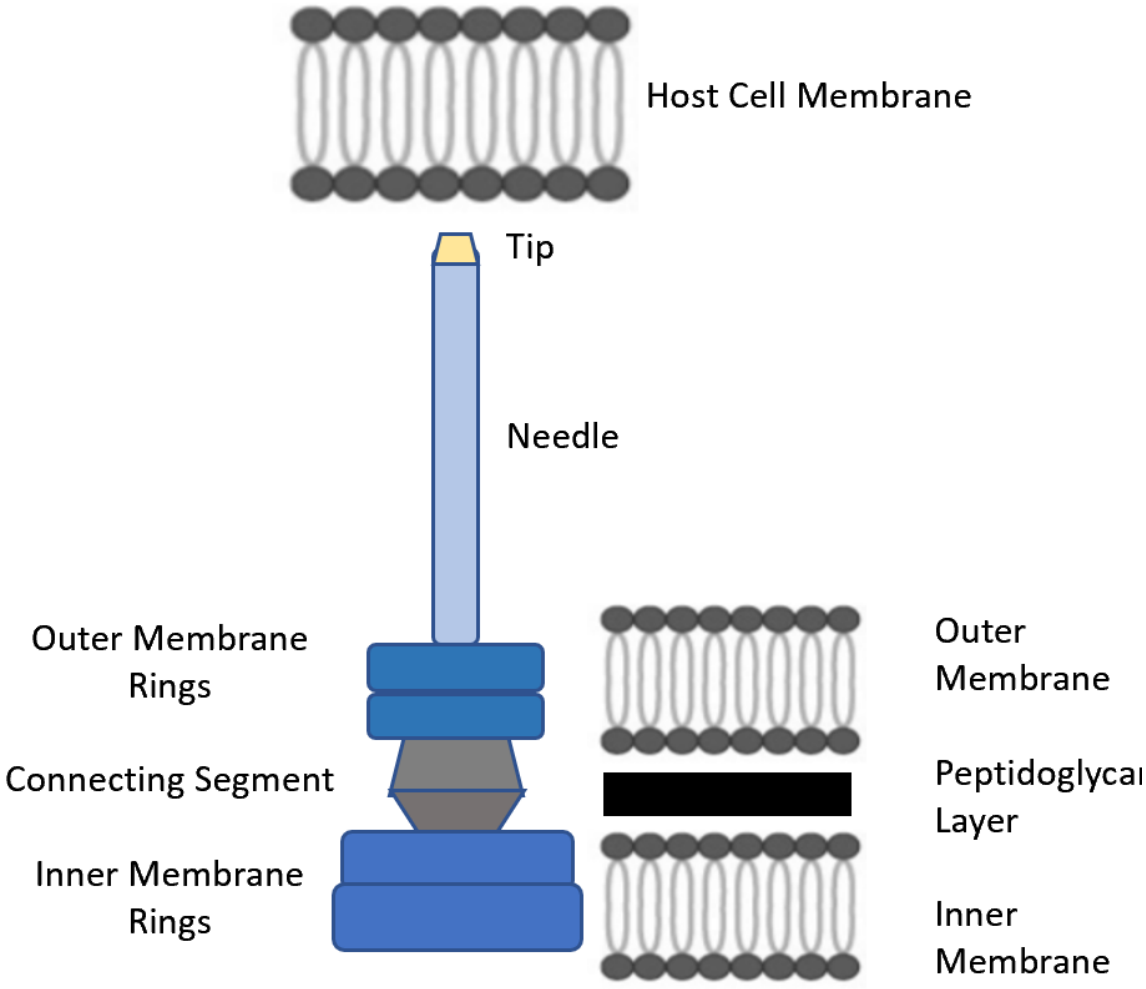

Figure 1: Structure of Type-III Secretion Systems.

1.1 Type-III Secretion Systems:

The T3SS injectosome apparatus consists of several different proteins that form basal body rings, a connecting segment and a needle [24]. The hydrophobic rings position the structure in the cell membranes of the bacterium, as well as the membrane of the host cell. The needle is composed of many subunits of a single protein that come together to form a tubular structure through which effector proteins pass into the host cell [24]. At

the very base of the basal body lies an export gate whose job is to open and close to allow the BEPs to flow through. The exact trigger that controls the opening of the export gate is not yet known; however, it does require that the needle contact the host cell membrane [24, 25].

1.2 Bacterial Effector Proteins:

Injections from some bacterial species contain only a few effectors, while other species inject up to several hundred different proteins at a time. Bacterial effector proteins perform a wide variety of roles once inside the mammalian cell, but all are intended to aid in bacterial survival. Many bacterial effectors do this by shutting down host defense systems like the transcription of antimicrobial peptides or the induction of inflammation. While others function to kill the host cell so that the bacterium can absorb its nutrients.. Many BEPs modulate apoptotic pathways to induce apoptosis in a variety of cell types. These effectors are almost always crucial for virulence and gene knockout results in complete avirulence.

The pathogen responsible for plague diseases, *Yersinia pestis*, has been shown to contain 14 bacterial effector proteins. The most well studied of these effectors is YopJ, a protein that is capable of modulating MAPK pathways and inducing apoptosis in a variety of mammalian cells. Another protein in the YopJ family, VopA is found in *Vibrio* species and performs many of the same functions as YopJ, but is less effective at inducing apoptosis. This study focuses primarily on these two proteins and their potential as cancer therapeutics.

1.3 Canonical MAPK Signaling:

The MAPK pathway regulates cell growth, division, differentiation, stress response and apoptosis through signaling cascades that result in the activation of transcription factors and other protein kinases [11, 12]. These cascades are composed of three families of mitogen-activated protein kinases: MAP3Ks, MAPKKs and MAPKs [12]. MAP3Ks are activated via phosphorylation by cell surface receptors after they have detected external stimuli and undergone a conformational change. These external stimuli include bacterial byproducts and growth factors. Once activated by the cell surface receptor, MAP3Ks activate MAPKKs. The now active MAPKKs go on to activate MAPKs. Once active, MAPKs work together to modulate the aforementioned cellular functions by activating and repressing the transcription of various proteins as well as activating many enzymes directly [11, 12].

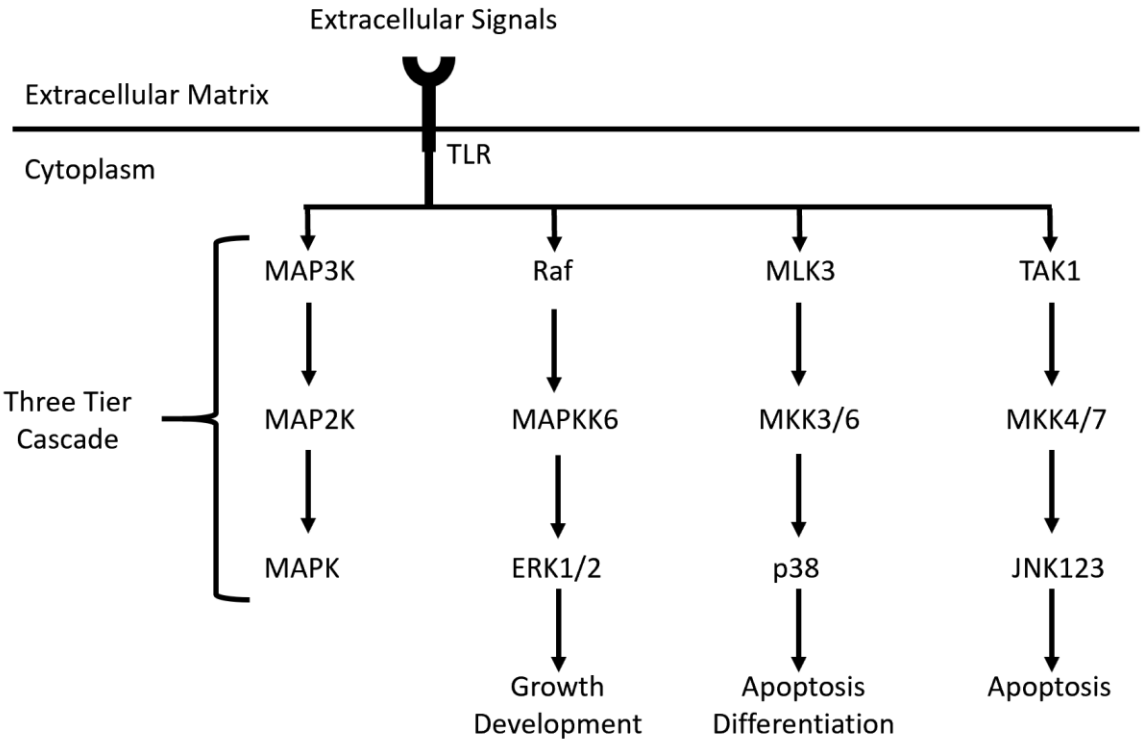

Figure 2: Canonical MAPK Signaling Pathways.

Mitogen-activated protein kinases are serine/tyrosine specific and their targets contain an activation loop motif with a serine and tyrosine that must both be phosphorylated for the enzyme to become active.

MAPK pathways are incredibly complex and often cross-talk between one another. This means that the activation of one kinase can lead to a variety of different effects. Often times, one kinase will activate multiple signaling intermediates, resulting in the simultaneous activation and repression of a single cellular mechanism like apoptosis. Since the activation of one enzyme can lead to the activation of multiple pathways that

oppose one another, the resulting cellular action is often determined by the degree to which each pathway is stimulated. Therefore, rather than working like an on/off switch, many cellular mechanisms that are controlled by the MAPK signaling pathway function on an intensity scale [43].

1.4 YopJ and VopA Modulation of the MAPK Pathway:

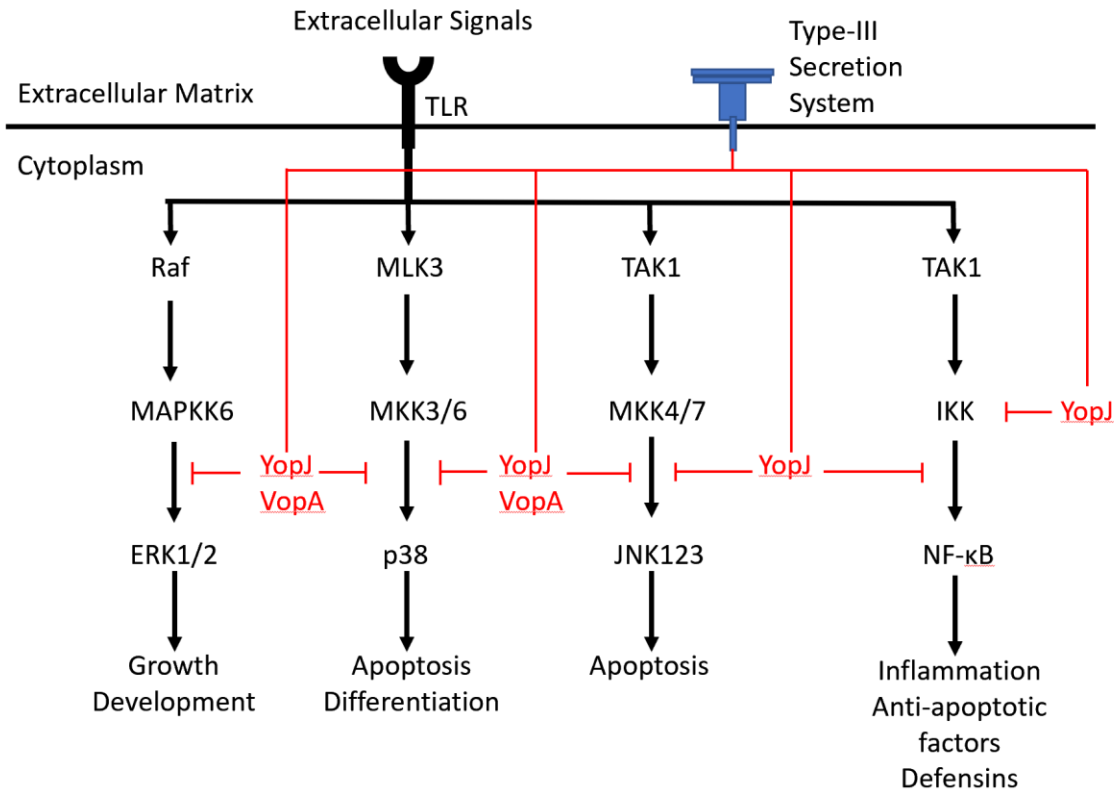

Figure 3: YopJ Activation of MAPK Pathways.

VopA and YopJ are bacterial effector proteins that are found in *V. parahaemolyticus* and *Yersinia pestis* species, respectively, that interrupt MAPK signaling cascades by acetylating several MAPKKs, including ERK, p38 and JNK [Figure 3]. In the absence of YopJ and VopA, toll-like receptors (TLRs) on the cell surface would detect the presence of bacterial byproducts and recruit Raf, MLK3 and TAK1. These MAP3Ks would continue the phosphorylation cascade resulting in downstream effects that decrease cell growth and differentiation, while increasing

YopJ and VopA acetylate MAPKKs in order to stop the signaling cascade before it is able to initiate a defensive against the bacteria. YopJ has been shown to acetylate the activation loop of MAPKK6 with the help of acetyl coenzyme A (Acetyl CoA) [23]. In this way, YopJ mediated acetylation directly competes with phosphorylation. Through this mechanism, YopJ slows or inhibits MAPK signaling pathways in order to facilitate bacterial evasion of host elimination [1, 2, 3].

1.5 Canonical Apoptotic Signaling:

Apoptosis is programmed cell death and can occur as a result of many different triggers. It is initiated in many tissues during development when structures must be formed by the removal of cells from an area. For example, the hand develops first with webbed fingers until apoptosis is initiated in specific cells, removing tissue from the space between each bone to allow the formation of fingers [46]. Apoptosis can also be initiated in response to viral infection in order to kill off infected cells to attempt to stop

the spread of the virus [47]. Apoptosis is less common under conditions of bacterial infection, but some gram-negative bacteria utilize bacterial effectors to initiate apoptosis in immune cells to avoid elimination [2, 10].

Apoptotic signaling is dependent on caspases; proteins that activate one another through cleavage and initiate signaling cascades that result in the transcription of cell-death genes and the release of cytotoxic molecules. Apoptotic signaling can be split into two major pathways, the intrinsic and extrinsic pathways [46, 48].

The intrinsic apoptotic pathway is canonically triggered by interactions within the cell. This pathway is most often activated by molecules that are able to cross the cell membrane, radiation (DNA damage), hypoxia or a lack of growth factors [46]. When one of these triggers is detected, proteins called Bax and Bak come together to form pores in the mitochondrial membrane [48]. These pores allow for the release of cytochrome C. Cytochrome C then forms a complex with procaspase-9 and Apaf-1 called the apoptosome. The apoptosome is responsible for cleaving procaspase-9 into its active form, caspase-9, which then cleaves procaspase-3 into caspase-3. Caspase-3 is known as the major effector caspase because it is responsible for carrying out functions such as initiating the transcription of proteins that lead to cell death [46, 48].

The extrinsic apoptotic pathway is activated by a wide variety of extracellular ligands that bind to death receptors on the outside of the cell, causing a conformational change [46]. This conformational change results in the recruitment of the DISC complex. procaspase-8 binds to the DISC complex, is cleaved and dimerizes to form caspase-8. caspase-8 then cleaves procaspase-3 into caspase-3. Thus, both the intrinsic and extrinsic apoptotic pathways result in caspase-3 activation and rely on its ability to induce cell

death. Caspase-8 has a second function that is to cleave tBID into BID. BID then oligomerizes Bak which, together with Bax [46], forms pores in the mitochondrial membrane, initiating the intrinsic apoptotic pathway. Thus, activation of the extrinsic apoptotic pathway results in the downstream activation of the intrinsic apoptotic pathway [46, 49].

1.6 YopJ Modulation of Apoptotic Signaling:

In addition to modulating MAPK signaling, YopJ has also been shown to activate both the intrinsic and extrinsic apoptotic pathways [22]. It first initiates the extrinsic apoptosis pathway by activating the death receptor, DISC or Procaspase 8; leading to the activation of caspase 8. Caspase 8 then truncates BID to activate the intrinsic pathway [Figure 4]. Prior experiments have shown that the YopJ mechanism of apoptotic induction is rapid and efficient [2]. Because of this ability, it was selected as the major effector to deliver into cancer cells in our experiments.

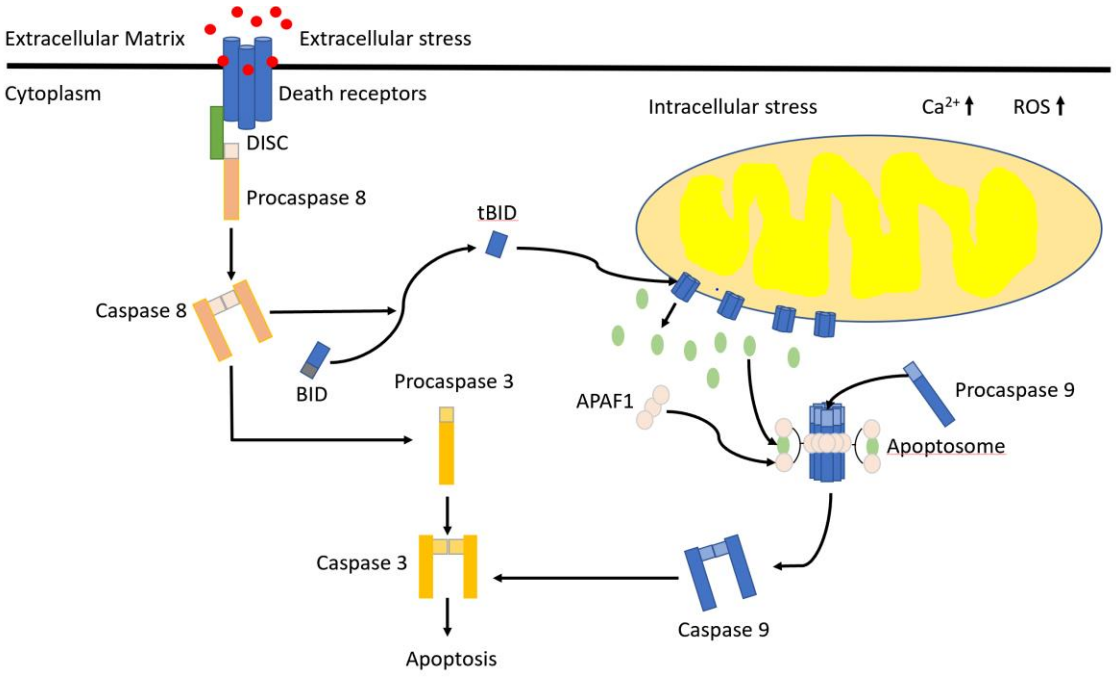

Figure 4: YopJ Activation of the Apoptotic Pathway. Original Image modified from Galluzzi et al., 2009 [6]. YopJ has been reported to activate the extrinsic apoptotic pathway by internally stimulating the death receptor or by activating caspase-8 directly [22].

1.7 The TAT-CaM Adaptor System:

Cell penetrating peptides are short peptide sequences that can cross the cell membrane. Our technology was developed around TAT, a CPP that is native to the HIV virus. A wide variety of cargo proteins can be bound to TAT and pulled into the cell with it. The problem with ordinary CPP delivery is that the cargo remains attached to TAT and cannot escape the endosome that TAT is bound to after endocytosis [5]. Our technology overcomes the obstacle of endosomal entrapment by incorporating calcium-dependant binding through a protein called calmodulin (CaM) [Figure 6]. CaM is attached

covalently to TAT just like any other cargo. However, a user defined cargo protein encoded with a Calmodulin Binding Site (CBS) can then be bound to CaM in a calcium dependent fashion. Calmodulin binds the cargo tightly in the presence of calcium but releases the cargo when calcium concentrations are low. Since intracellular concentrations of calcium are natively low, this mechanism works very well for the delivery of cargo into cells [4, 5]. The TAT-CaM complex binds tightly to the cargo outside of the cell where calcium concentrations are high. Once the complex enters the cell in an endosome, calcium inside the endosome begins to flow down the concentration gradient and into the cytoplasm, which has a lower calcium concentration than the extracellular environment. Once calcium concentrations drop to a low enough level within the endosome, the CBS tag on the cargo protein no longer binds tightly to TAT-CaM and the cargo protein is released into the cytoplasm of the cell, while TAT-CaM remains bound to the endosomal membrane [Figure 6] [4, 5].

A.

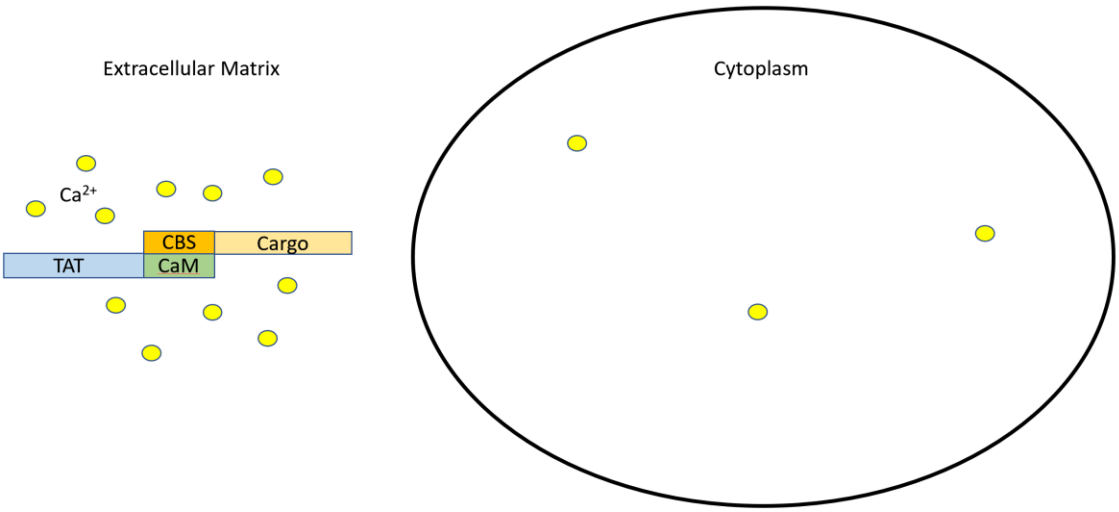
Extracellular Matrix
Cytoplasm
Ca2+
CBS
Cargo
TAT
CaM

B.

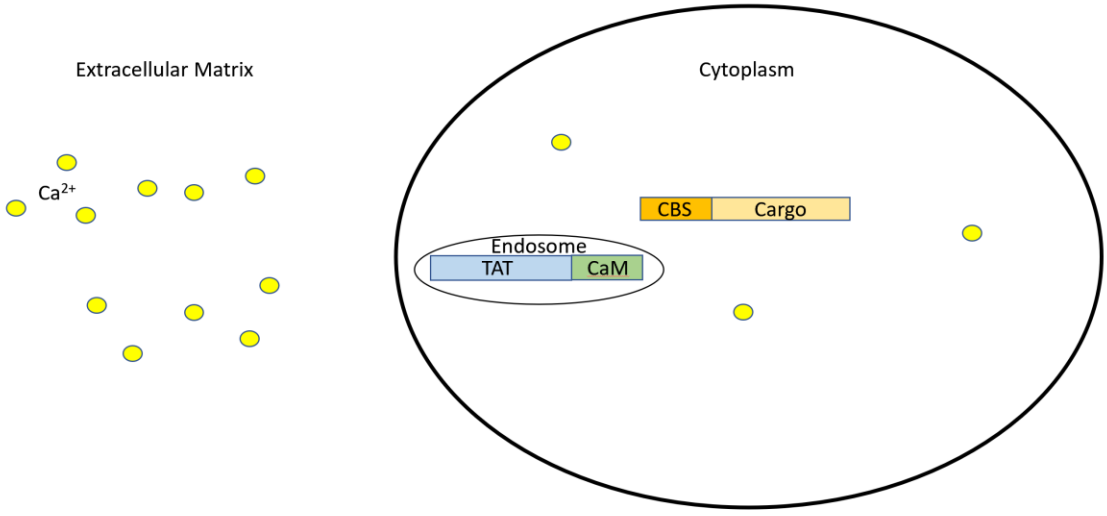
Extracellular Matrix
Cytoplasm
Ca2+
CBS
Cargo
Endosome
TAT
CaM

Figure 5: The TAT-CaM Adapter System. A. Calmodulin binds tightly to the CBS tag on the protein in the presence of calcium. **B.** Calmodulin dissociates from the CBS tag on the cargo protein as endosomal calcium levels lower and approach homeostasis with the internal cellular environment.

Our goal is to utilize this TAT-CaM system to deliver bacterial effector proteins YopJ and VopA into the cytoplasm of cancer cells, where they have been shown to induce apoptosis [1, 2, 3]. We believe that our system will be an effective method of delivery as it has been shown to work in the past with other cargos of various sizes and structures [4, 5].

2. ANALYSIS, EXPRESSION AND PURIFICATION OF TAT-CAM AND BACTERIAL EFFECTORS

2.1: Introduction:

We propose a method for the cytoplasmic delivery of bacterial effector proteins VopA and YopJ to colon cancer cells in order to interrupt the MAPK pathway. Based on previous research by Rheinallt M. Jones et al. [2, 3], we believe that this will initiate apoptosis, resulting in the death of the colon cancer cells. Although these proteins have been shown to inhibit the MAPK pathway resulting in reduced cell growth, they have not been utilized against cancer cells due to the lack of an efficient delivery mechanism that does not require infection by a bacterial pathogen. We hope to overcome this obstacle by utilizing cell penetrating peptide (CPP) technology [4, 5].

In order to begin our experiments, we needed to prepare pure TAT-CaM, as well as pure effector proteins containing the CBS tag. In addition to purifying the YopJ protein, we analyzed it using several bioinformatics tools to further understand how it works.

2.2 Materials and Methods:

2.2.1 Construction of TAT-CaM Expression Vector:

To generate pure protein for use in experiments, the protein expression vector constructed by Salerno et al. was utilized [5].

2.2.2 Construction of Bacterial Effector Expression Vectors:

To generate pure protein for use in experiments, a protein expression vector was constructed and ordered from GeneWiz [50]. The pET-19b vector was modified with a 6-residue histidine tag for purification and the gene of interest at the N-terminus. The gene of interest was cloned into the vector using *Nde*I and *Bam*HI restriction endonuclease sites.

2.2.3 Transformation of Plasmid into Nova Blue and BL21 (DE3) Cells:

We received 2μg of lyophilized plasmid containing the desired construct. The plasmid was then dissolved in elution buffer (10 mM Tris-HCl, pH 8.5 and 0.1 mM EDTA). Frozen competent cells were thawed on ice for 5 to 10 min. After the addition of 50-100ng of plasmid DNA to the competent cells, they were incubated on ice for 30 minutes. The cells were then placed in a 42°C heat bath for 1 minute before being transferred to an ice bucket for 2 minutes. 1mL of Luria-Bertani (LB) broth was added to the cells and they were incubated at 37°C for 1 hour, while shaking. The cells were then concentrated to a volume of 150uL and were plated on an ampicillin/tetracycline resistant LB agar plate and incubated overnight at 37°C. Overnight cultures of Nova Blue cells were prepared in order to maintain stocks of DNA. These cultures were prepared by inoculating 5mL of LB medium with a single fresh colony and this was allowed to grow overnight at 37°C, shaking at 220rpm. DNA was then mini-prepped from these cells to obtain pure samples.

2.2.4 Expression of TAT-CaM:

An overnight culture was prepared by inoculating 50mL of LB medium (containing ampicillin and chloramphenicol) with a single fresh colony and allowing it to grow overnight at 37°C. In the morning, 10mL of this culture was added to 1L of LB medium (containing ampicillin and chloramphenicol) and allowed to grow at 37°C. Optical density measurements were taken until the culture achieved an absorbance level between 0.4 and 0.6 when read at 600nm. The temperature was lowered to 30°C and the cells were induced with 0.2 mM isopropyl-1-thio-β-D-galactopyranoside (IPTG, Sigma-Aldrich). Cells were induced for 4-6 hours before harvesting. Cultures were harvested using a Sovall R 5C plus centrifuge spinning at 7000 rpm at 4°C before being decanted and stored at -80°C for later purification.

2.2.5 Expression of Bacterial Effectors:

An overnight culture was prepared by inoculating 50mL of LB medium (containing ampicillin and chloramphenicol) with a single fresh colony and allowing it to grow overnight at 37°C. In the morning, 10mL of this culture was added to 1L of LB medium (containing ampicillin and chloramphenicol) and allowed to grow at 37°C. Optical density measurements were taken until the culture achieved an absorbance level between 0.4 and 0.6 when read at 600nm. The temperature was lowered to 25°C and the cells were induced with 0.2 mM isopropyl-1-thio-β-D-galactopyranoside (IPTG, Sigma-Aldrich). Cells were induced for 4-6 hours before harvesting. Cultures were harvested

using a Sovall R 5C plus centrifuge spinning at 7000 rpm at 4°C before being decanted and stored at -80°C for use in purification.

2.2.6 Purification of TAT-CaM and Bacterial Effectors:

Cells were resuspended in 25mL of lysis buffer (10mM Tris-base pH 8.0, 10mM imidazole, 0.05% Tween, 500mM NaCl, 10% glycerol) with the help of a vortex and a homogenizer. DNase and lysozyme were added to break down DNA and cell membranes, respectively. The homogenized lysates were then run through a French press to rupture the cell membranes and release cellular contents into the supernatant. The lysates were then separated into supernatant and lysate pellets by centrifugation at 18,000 rpm. Proteins in the soluble supernatant were purified by His-tag affinity chromatography. Talon metal affinity resin (ClonTech laboratories, CA, USA) was used according to the manufacturer's instructions. 3mL of resin/storage solution mixture was centrifuged to remove the storage solution. Then, the resin was equilibrated in lysis buffer (10mM Tris-base pH 8.0, 25mM imidazole, 0.05% Tween, 500mM NaCl, 10% glycerol) by washing three times with 3mL. The resin was then resuspended in 3mL of lysis buffer added to the supernatant and rocked at 4°C for 45 minutes to allow binding to occur. The protein-resin complex was then poured into a gravity column and washed with 10mL of wash buffer (10mM Tris-base pH 8.0, 25mM imidazole, 0.05% Tween, 500mM NaCl, 10% glycerol) three times. The protein of interest was then eluted with elution buffer (10mM Tris-base pH 8.0, 250mM imidazole, 0.05% Tween, 500mM NaCl, 10% glycerol) in ten 1mL elutions. Excess salts were removed from the product via FPLC buffer exchange through

a desalting column into NEB buffer (10mM Hepes, 150mM NaCl, 1mM $CaCl_2$, 10% Glycerol, 1mM DTT). Purified protein products were stored at -80°C.

2.3 Results and Discussion:

In order to better understand the functionality of YopJ, it was analyzed using Jpred4 and Scansite. This software identified the predicted secondary structure of YopJ as well as two active sites in the protein. The first is a phosphoserine/threonine binding site and the second is a kinase binding site. These two sites help to confirm the theory that YopJ is a serine/threonine acetyltransferase that acts on kinases.

A.

```
        10         20         30         40         50
MIGPISQINI SGGLSEKETS SLISNEELKN IITQLETDIS DGSWFHKNYS
        60         70         80         90        100
RMDVEVMPAL VIQANNKYPE MNLNLVTSPL DLSIEIKNVI ENGVRSSRFI
       110        120        130        140        150
INMGEGGIHF SVIDYKHING KTSLILFEPA NFNSMGPAML AIRTKTAIER
       160        170        180        190        200
YQLPDCHFSM VEMDIQRSSS ECGIFSFALA KKLYIERDSL LKIHEDNIKG
       210        220        230        240        250
ILSDGENPLP HDKLDPYLPV TFYKHTQGKK RLNEYLNTNP QGVGTVVNKK
       260        270        280
NETIVNRFDN NKSIVDGKEL SVSVHKKRIA EYKTLLKV
```

B.

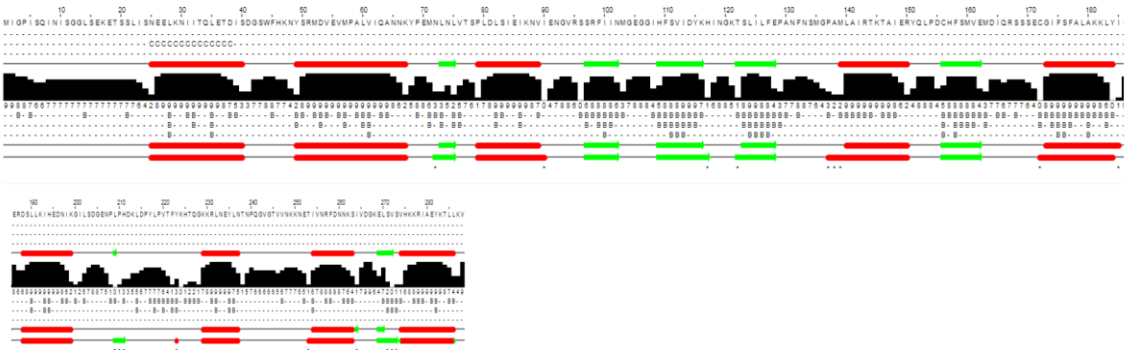

C.

0.423	0.672%	14-3-3 Mode 1 (1433_m1)	Phosphoserine/threonine binding group (pST_bind)	S170	MDIQRSSeECGIFSF	0.5067	YWHAZ 1433Z_HUMAN	cytoplasm
0.606	0.971%	PDK1 Binding (PDK1_Bind)	Kinase binding site group (Kin_bind)	S176	SSECGIFeFALAKKL	0.1345	PDPK1 PDPK1_HUMAN	nucleus

Figure 6: Structural Analysis of YopJ. A. DNA sequence of *Yersinia pestis* YopJ acquired via UniProt. **B**. Secondary structure prediction acquired via Jpred4 [45]. Helices in red, B-sheets in green. **C**. Functional domain prediction using Scansite [44]. A phosphoserine/threonine binding site and a kinase binding site were identified. This supports the theory that YopJ has serine/threonine acetyltransferase activity towards kinases in the MAPK pathways.

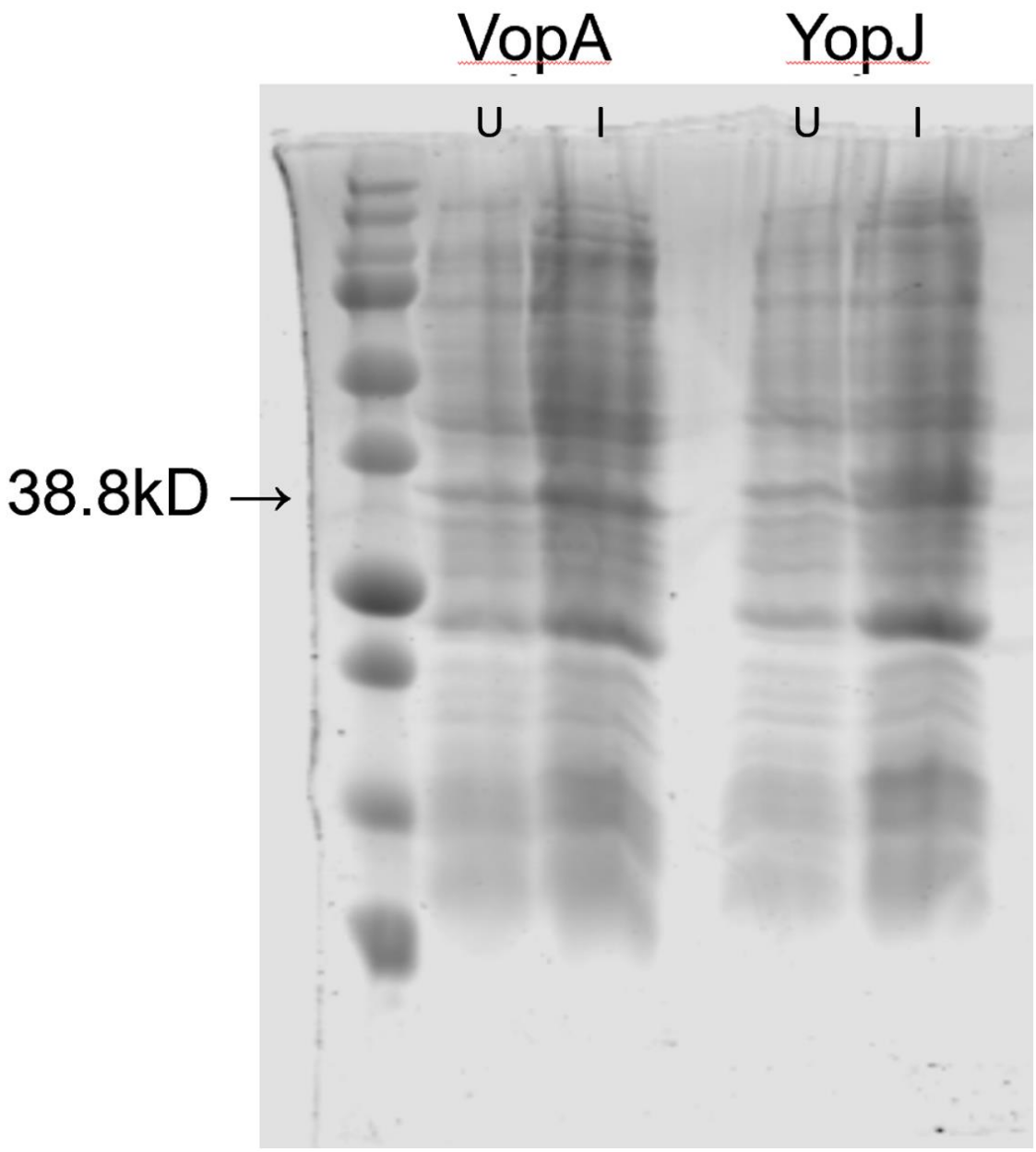

Figure 7: Expression of YopJ and VopA. The molecular weight marker used is Precision Plus Protein Dual Color [51]. The first two lanes show VopA expression, the third and fourth two lanes show YopJ expression. Lanes marked "U" are uninduced and should not show a band at the indicated size. Lanes marked "I" contain samples that have been induced and a band should appear at 38.8kD. Expression of VopA was unsuccessful and very small amounts of the protein were produced. Expression of YopJ was more effective and a band can be seen at 38.8kD. However, neither proteins were expressed in large amounts.

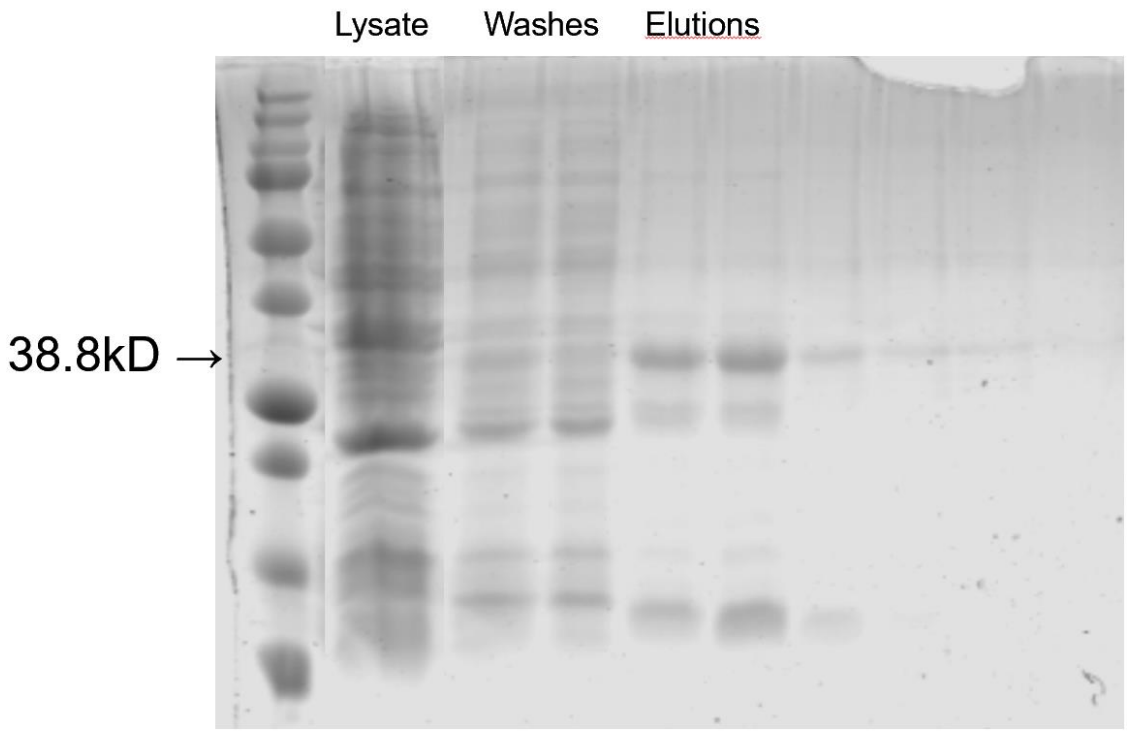

Figure 8: Purification of Effectors (YopJ). The molecular marked used is Precision Plus Dual Color Standard [51]. Full length protein can be seen at 38.8kD. However, two breakdown products were copurified.

Effector purification proved to be far more difficult than anticipated. Breakdown products that contained the His-Tag were purified alongside of the full-length protein. These products can be seen in the elutions of Figure 8. In an attempt to reduce the amount of breakdown product present, all purification steps were performed in a room that maintains 4°C and with the addition of 2mM 2-Mercaptoethanol as a reducing agent. These breakdown products were present in all protein preps [Figure 8].

3. BIO-LAYER INTERFEROMETRY AND INTRACELLULAR DELIVERY ASSAY

3.1 Bio-Layer Interferometry:

Biolayer interferometry is a biosensing technique that operates in real time. One molecule, the ligand is tethered at the tip of the optical biosensor. White light travels down to the molecule and reflects off. The interference pattern is measured as a shift in wavelength. Once a baseline has been established, the senor is then moved into an analyte containing buffer to monitor association and finally moved into an analyte free buffer to measure dissociation. Binding of both the ligand and the analyte on the sensor increases the reflecting surface hence causing a coincident change in the interference pattern

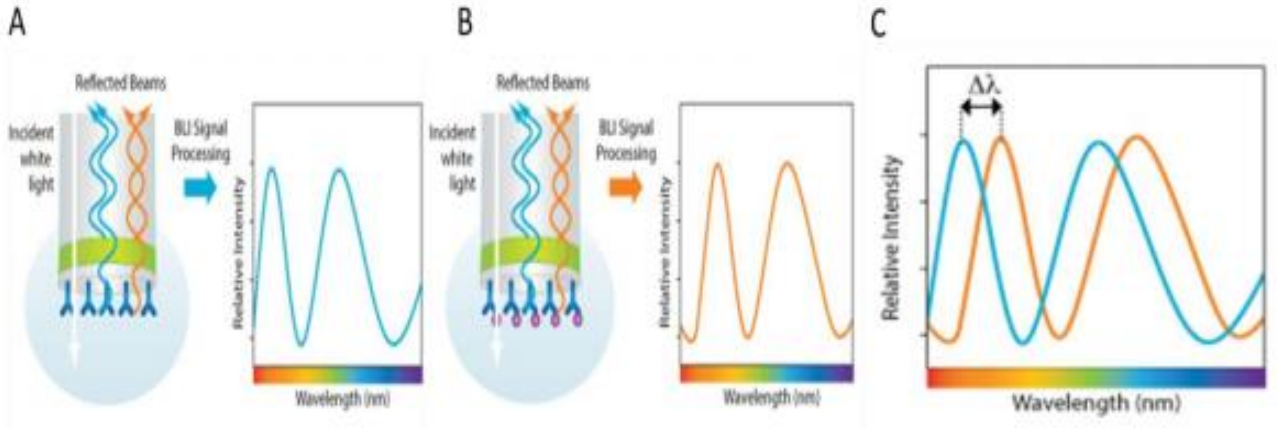

Figure 9: Biolayer Interferometry. A. An interference pattern is established by reflection of white light from two surfaces on a fiber optic sensor with biotinylated molecules attached to the biolayer. **B.** Binding of analyte molecules causes a shift in the wavelength of the interference pattern. **C.** Monitoring of the interference shift over time reflects association of analyte with the immobilized molecule. Association is measured in

the presence of analyte and dissociation is measured when the sensor is moved to buffer containing no analyte. Image from ForteBio.com.

The kinetics of the TAT-CaM-Cargo system were assessed via bio-layer interferometry using a FortéBio Octet QK biosensor with treptavidin sensors (SA). Assays were performed in black 96-well microplates at 25°C. All volumes were 200µL. TAT-CaM was biotinylated using NHS-LC-LC-biotin (succinimidyl-6-[biotinamido]-6-hexanamidohexanoate) (Thermo Scientific, Rockford, IL, USA) at a 10:1 molar ratio of biotin to protein for 30 min at 25°C. Biotinylated TAT-CaM was then loaded onto the streptavidin sensor and a baseline of the interference pattern was established prior to associating ananalyte (CBS-YopJ). Dissociation was subsequently analyzed by moving the sensor to a well that contained no free analyte to determine how well the complex stays together Next, the sensor was moved to a well containing 10mM EDTA to mimic the low calcium environment of the inside of the cell, in which the complex should dissociate.

3.2 Eukaryotic Cell Culture:

Starting BHK 21 and SiHa (HTB-35) ATCC Cell Lines:

Cells were removed from liquid nitrogen storage and placed in a 37°C bead bath for 2 minutes and then warmed in the hand and closely monitored until they thawed. The cells were then transferred into a 15mL conical tube containing 5mL of Dulbecco's modified Eagle's medium (DMEM) containing 10% fetal bovine serum (FBS). Cells were centrifuged for 5 minutes at 1000 rpm at 30°C. Cells were then re-suspended into

12mL of pre-warmed growth media at 37°C and then transferred into a T-75 flask. Cells were then returned into the incubator to be incubated at 37°C under 5% carbon dioxide atmosphere conditions.

Sub-culturing BHK and SiHa cells:

Cells were maintained as they grew through regular media changes. When cells were maximally between 80-90% confluent in a T-75 flask, the culture medium was removed and discarded. The cell layer was quickly rinsed with 0.25% (w/v) Trypsin-0.1% EDTA solution to remove all traces of serum which contains trypsin inhibitors. 1mL of Trypsin-EDTA solution was added into the flask and it was placed in the 37°C incubator for 5 minutes and cell dispersion was periodically observed under a light microscope. Once the cell population was detached from the surface of the flask, 9mL of growth media was added into the T-75 flask and was pipetted gently to mix. 2mL of the cells in suspension were added to a new T-75 flask containing 10mL of sterile growth media. Cells were also plated in chambered Lab-Tek 4-well cover glass slides (Fisher Scientific) at 50% confluence for intracellular delivery experiments.

3.3 Intracellular Delivery Assay:

Cells were seeded in three wells of a 4-well Lab-Tek chambered cover glass (Fisher Scientific) at 50% confluence in DMEM medium supplemented with 5% FBS and cultured overnight. The medium was discarded and replaced with fresh medium. TAT-CaM and CBS-Cargo were combined and allowed to incubate on ice for 5-10 minutes. The TAT-CaM Cargo complex was then diluted in media to a concentration of 1uM.

Cargo by itself was also diluted to 1uM in media. One well was treated with the TAT-CaM-Cargo complex, another was treated with the cargo alone and the third well was an untreated control. The chamber culture plate was incubated for 1 hour at 37°C in a 5% CO2 atmosphere. Cells were rinsed three times with PBS containing calcium and magnesium. The cells were treated with 2 µM cell tracker green dye (Thermo Fisher) for 20 min with incubation followed by three rinses with PBS. Cells were stained with a drop of NucBlue for 10min at 37°C. After three washes with PBS, DMEM/5% FBS medium containing 25mM HEPES pH7.4 buffer was added into the chambers. Penetration was analyzed using confocal microscopy.

3.4 Results and Discussion:

Before intracellular delivery assays could be performed, the functionality of the TAT-CaM-YopJ adaptor system had to be assessed. Biolayer interferometry was used to confirm this. As seen in figure 10, YopJ bound tightly to TAT-CaM in the presence of calcium and did not dissociate easily. However, figure 11 demonstrates that when calcium is removed from the environment, rapid dissociation of the complex occurs. Thus the system was working as intended *in vitro* and was expected to do the same *in cells*.

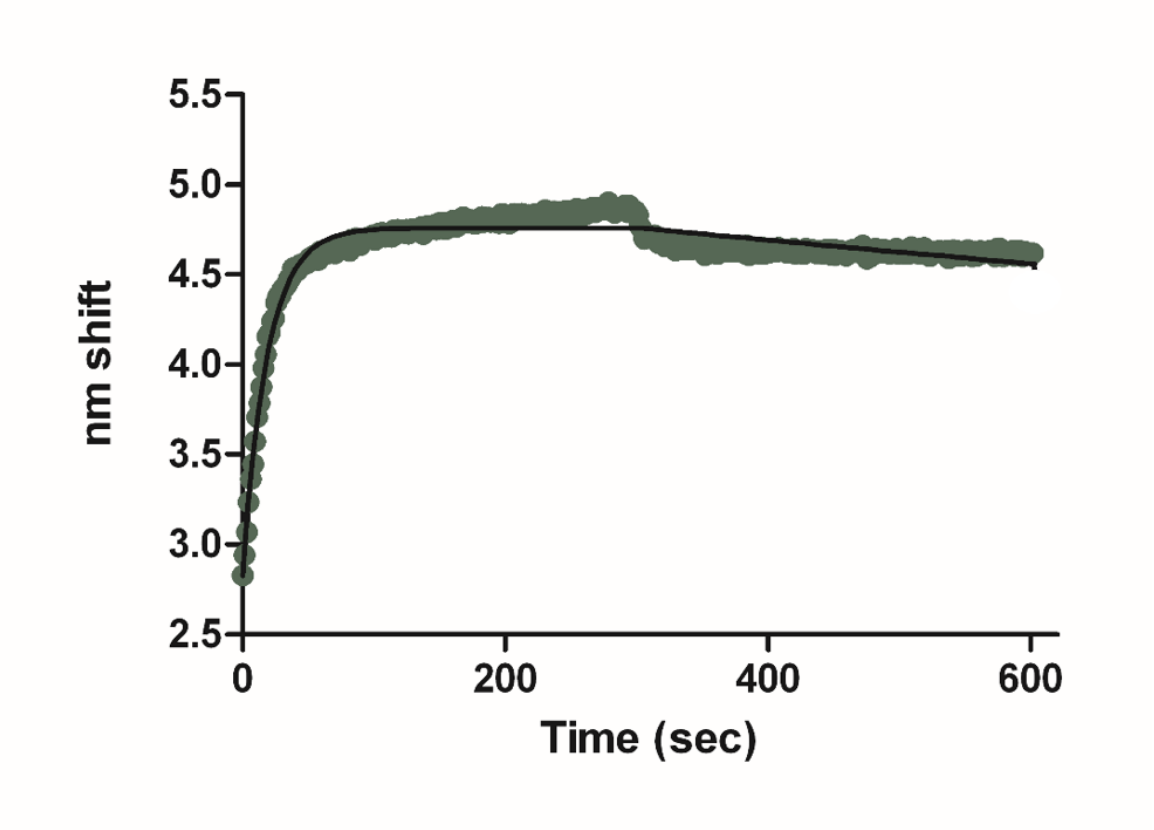

Figure 10: Association of YopJ to TAT-CaM. YopJ binds to TAT-CaM with high affinity in the presence of calcium. This data represents the change in the interference pattern recorded by the ForteBio Octet K2 when YopJ binds to TAT-CaM which is bound to a streptavidin sensor. Both proteins were present at 1uM in solution.

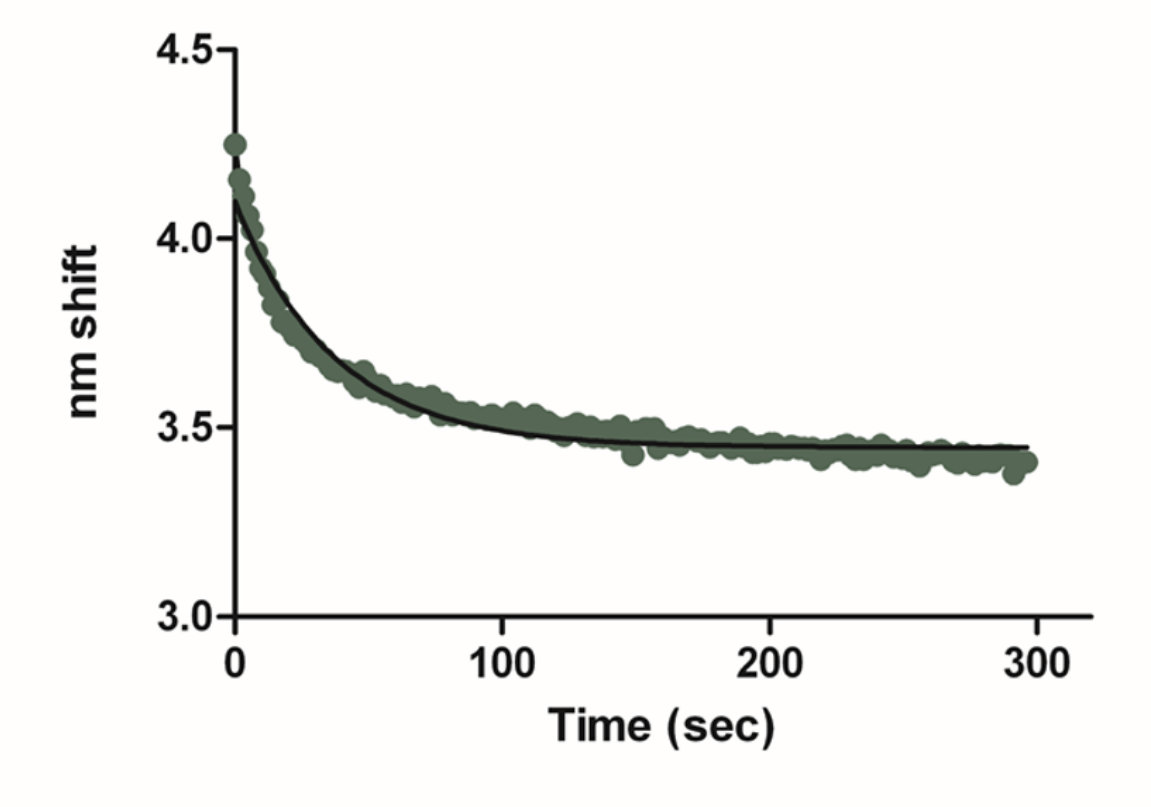

Figure 11: Dissociation of YopJ from TAT-CaM. YopJ rapidly dissociates from TAT-CaM in the absence of calcium. This data represents the shift in the interference pattern recorded by the ForteBio Octet K2 when YopJ releases from TAT-CaM which is bound to a streptavidin sensor upon introduction of 0.1mM EDTA. EDTA binds up the calcium in solution, mimicking the low calcium conditions found in the cytoplasm of eukaryotic cells. Both YopJ and TAT-CaM were present at 1uM in solution.

Many cellular delivery experiments resulted in the uptake of YopJ into the cell not only when it was bound to TAT-CaM. but also when cells were treated with YopJ alone [Figures 12 and 13]. It is possible that the cells were unhealthy and therefore had permissible membranes.

A.

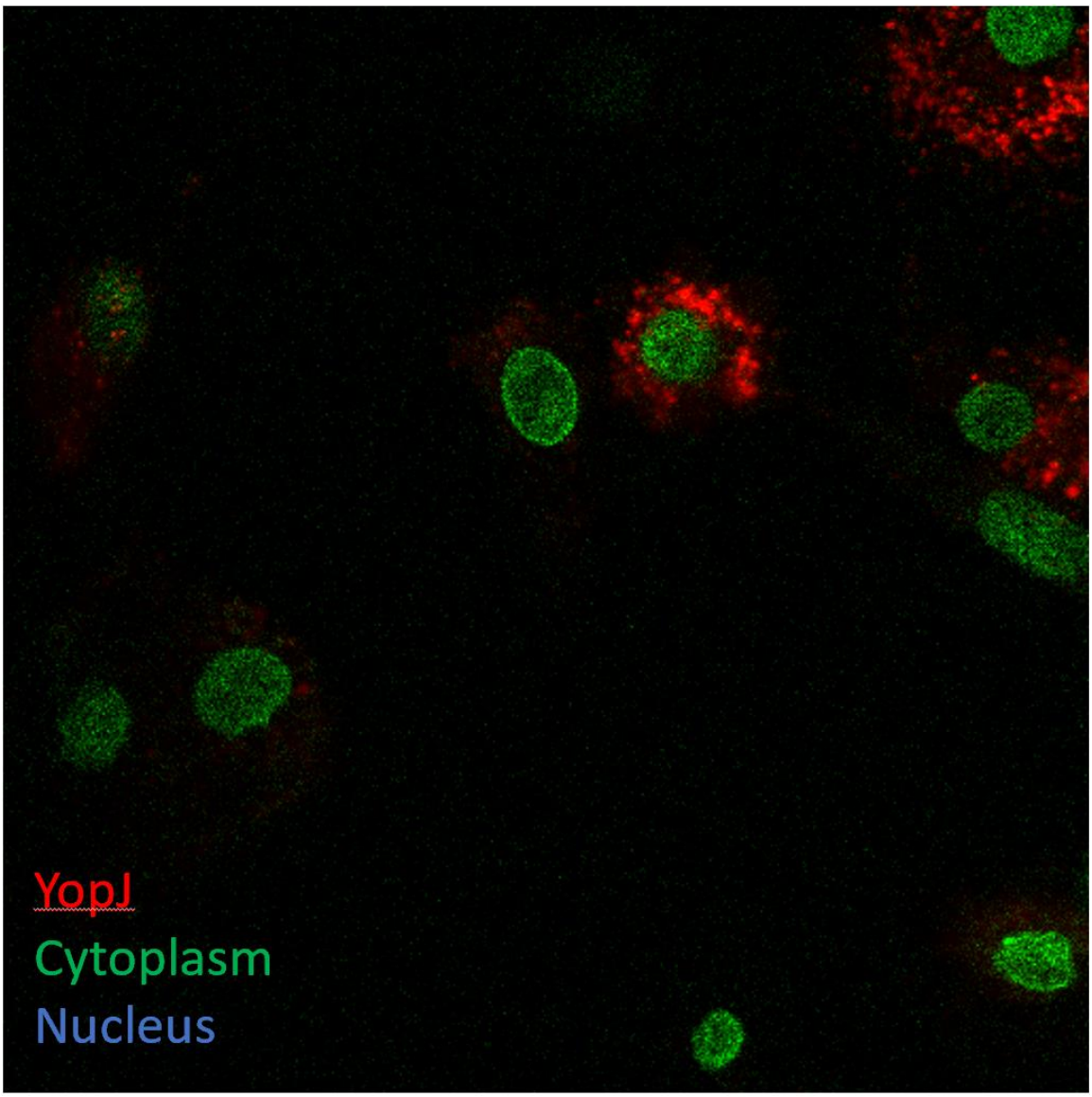

B.

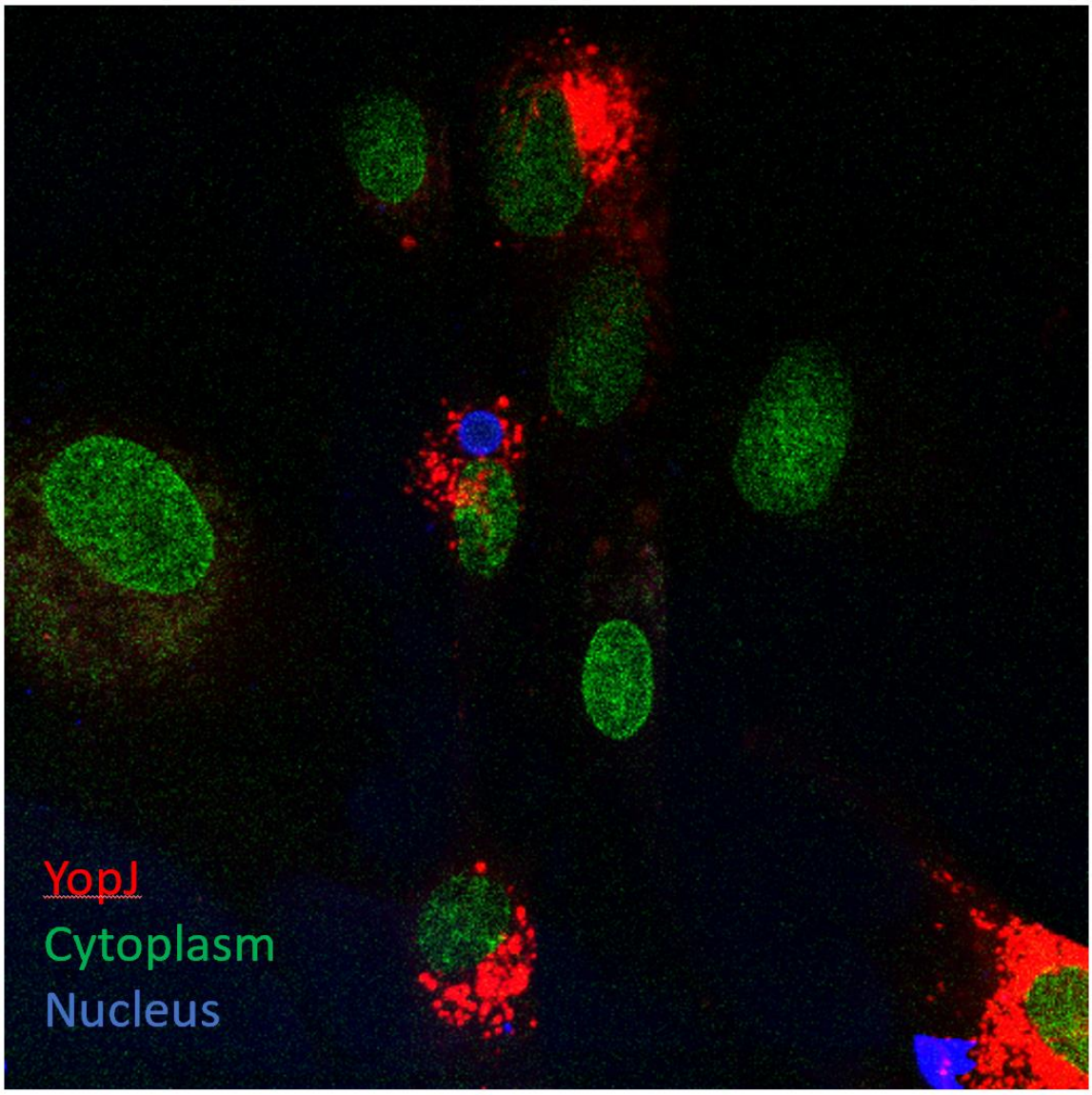

Figure 12: Uptake of YopJ into BHK cells in the absence of delivery vehicle. YopJ was labeled with DyLight 550 red fluorescent tag. The cytoplasm was stained with 1mM CellTracker Green (Thermo Fisher Scientific). The nuclei were stained with NucBlue LiveReady Probes (Thermo Fisher Scientific). The cytoplasmic dye can be seen entering the nucleus and the labeled YopJ entered the cytoplasm without a delivery vehicle. A and B represent two separate experiments with similar results.

Nuclear staining revealed that a bacterial infection was present in the BHK cell line. It is likely that these small bacteria were mycoplasma. Mycoplasma are a genus of small bacteria that lack cell walls surrounding their membranes and often enter into eukaryotic cells as parasites [52]. Due to the lack of a cell wall, they are unaffected by common antibiotics that target bacterial cell walls. Thus, in order to combat this contamination problem, all infected cells were thrown away, the hoods and culture materials were thoroughly disinfected, and new cell lines were started. However, further tests for mycoplasma showed that it was still present in some cells. The disinfecting of lab equipment and restarting of cell lines was performed several times until cells tested negative for mycoplasma.

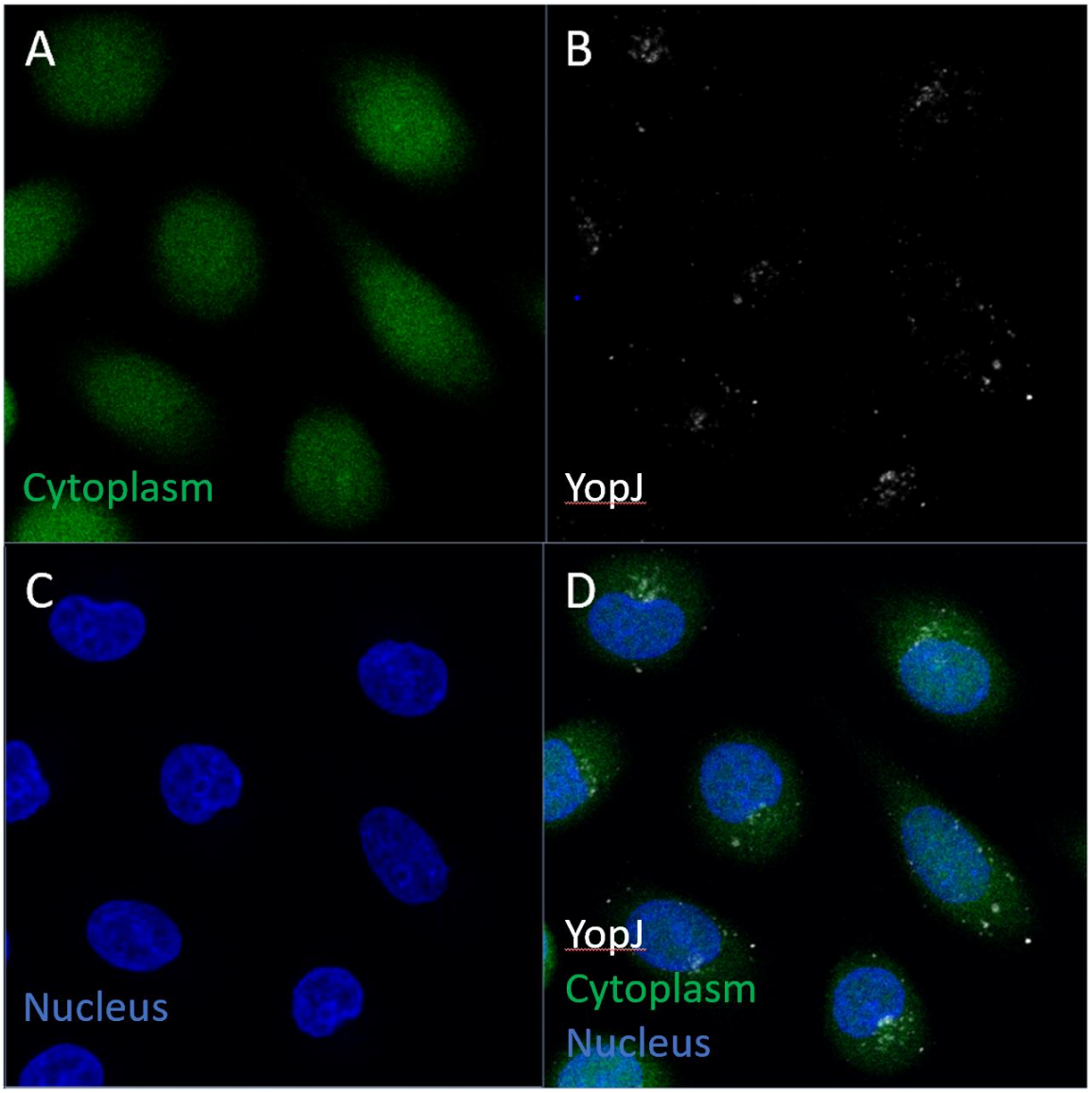

Figure 13: Uptake of YopJ in BHK cells. YopJ was labeled with DyLight 550 red fluorescent tag. The cytoplasm was stained with 1mM CellTracker Green (Thermo Fisher Scientific). The nuclei were stained with NucBlue LiveReady Probes (Thermo Fisher Scientific). YopJ is rendered in white. A. cytoplasm only. B. YopJ only. C. Nucleus only. D. Superimposed image of all three channels.

YopJ cellular delivery assays in BHK cells were performed once more after the mycoplasma infection was cleared. The cells looked haelthy and YopJ appeared to be entering the cell as it was expected to [Figure 13].

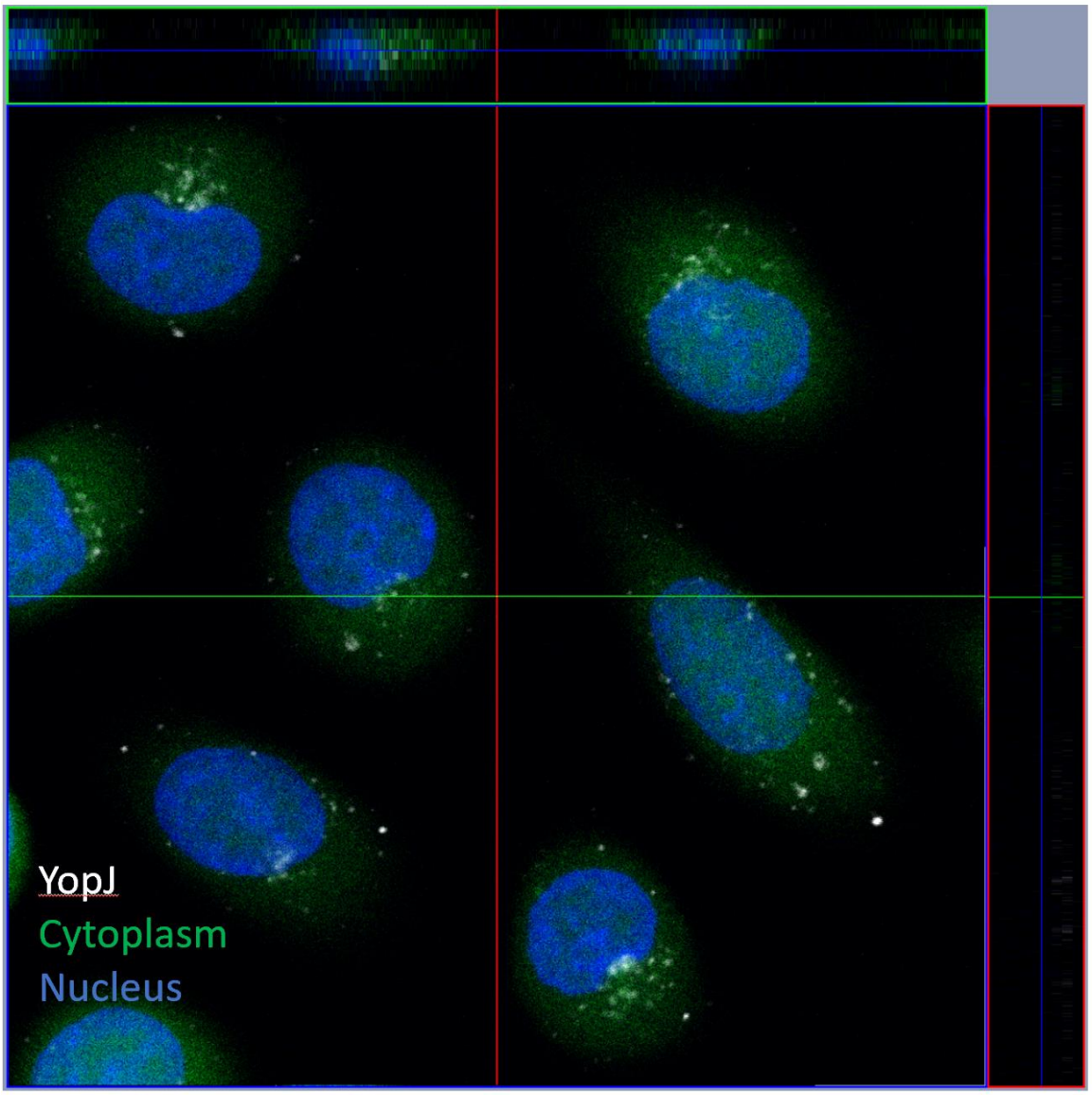

Figure 14: Orthogonal Projection of YopJ Uptake with TAT-CaM. This orthogonal projection shows the three-dimensional view of the cell. YopJ was labeled with DyLight 550 red fluorescent tag. The cytoplasm was stained with 1mM CellTracker Green (Thermo Fisher Scientific). The nuclei were stained with NucBlue LiveReady Probes (Thermo Fisher Scientific). YopJ is rendered in white.

In order to support the theory that that the protein was entering into the inside of the cell, a Z-stack was taken. This is a confocal microscopy technique in which several images are taken at different points along the Z-axis of the cell and the individual images are rendered in an orthogonal projection. This method allows one to look at each image to

determine if the protien is present at that depth in cell. The rendering in Figure 14 suggests that YopJ is likely inside the cell.

When the cells were unheathly, YopJ was able to enter into the cytopolasm without the help of TAT. A no TAT control was performed to see if YopJ would still be able to enter the cell without a delivery vehicle. Results were often mixed and YopJ was sometimes able to enter the cell without TAT-CaM and other times could not. In the experiments where YopJ entered without TAT-CaM, the cells were usually visibly unhealthy. When cells were healthy, YopJ entered the cells only in the presence of TAT-CaM [Figures 14 and 15 vs. Figures 16 and 17]. When the experiment was performed with healthy cells and in the absence of TAT-CaM, no protein can be seen within the cell.

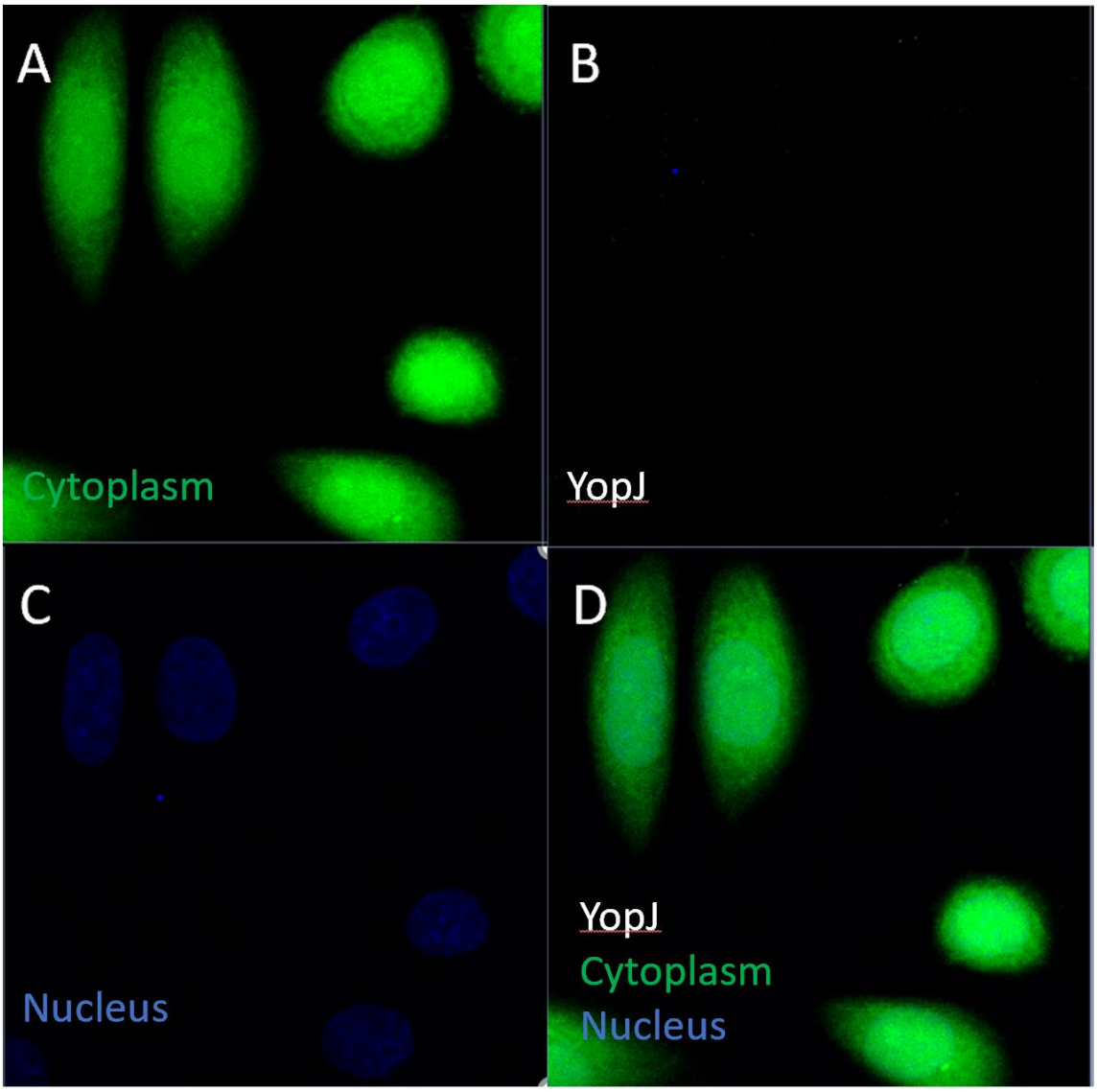

Figure 15: Uptake of YopJ in the Absence of TAT-CaM. YopJ was labeled with DyLight 550 red fluorescent tag. The cytoplasm was stained with 1mM CellTracker Green (Thermo Fisher Scientific). The nuclei were stained with NucBlue LiveReady Probes (Thermo Fisher Scientific). A. Cytoplasm only. B. YopJ only. C. Nucleus only. D. Superimposed image of all three channels.

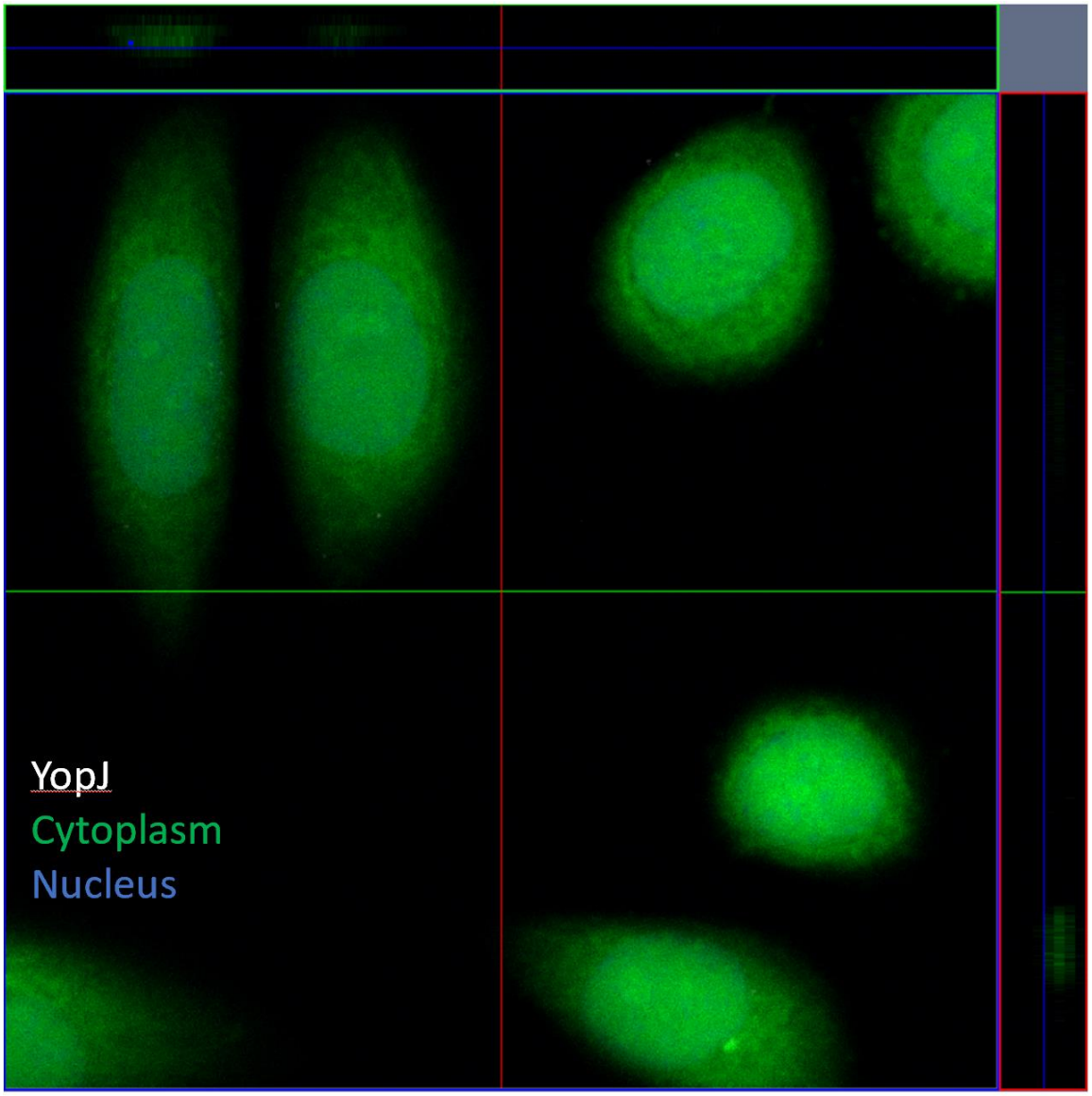

Figure 16: Orthogonal Projection of YopJ Uptake in the Absence of TAT-CaM. YopJ was labeled with DyLight 550 red fluorescent tag and was rendered in white. The cytoplasm was stained with 1mM CellTracker Green (Thermo Fisher Scientific).

These experiments were then repeated in SiHa cells, a human cervical cancer cell line, to determine whether or not YopJ could be delivered into epithelial cancer cells. Once again, YopJ was being taken up into the cells without the addition of TAT-CaM and the cells looked visibly distressed. A mycoplasma test revealed that the contamination was also in the SiHa cell line. So, the cells were discarded and the

laboratory equipment was disinfected. Several cycles of this disinfecting had to be performed before the cells tested mycoplasma-free.

Once the cells were clear of infection, the uptake assays were repeated in these cells. Figure 18 shows a side by side comparison of the delivery of YopJ by itself and YopJ in the presence of TAT-CaM in SiHa cells. Once again, the system was effectively delivering the protein into the cells only in the presence of TAT-CaM.

Despite obtaining positive results, data replication was a large obstacle. Cell health as well as other unknown factors caused the effector proteins to enter the cell without the presence of TAT-CaM. Perhaps with better cell culturing techniques and a more refined protocol, the assay would become more consistent.

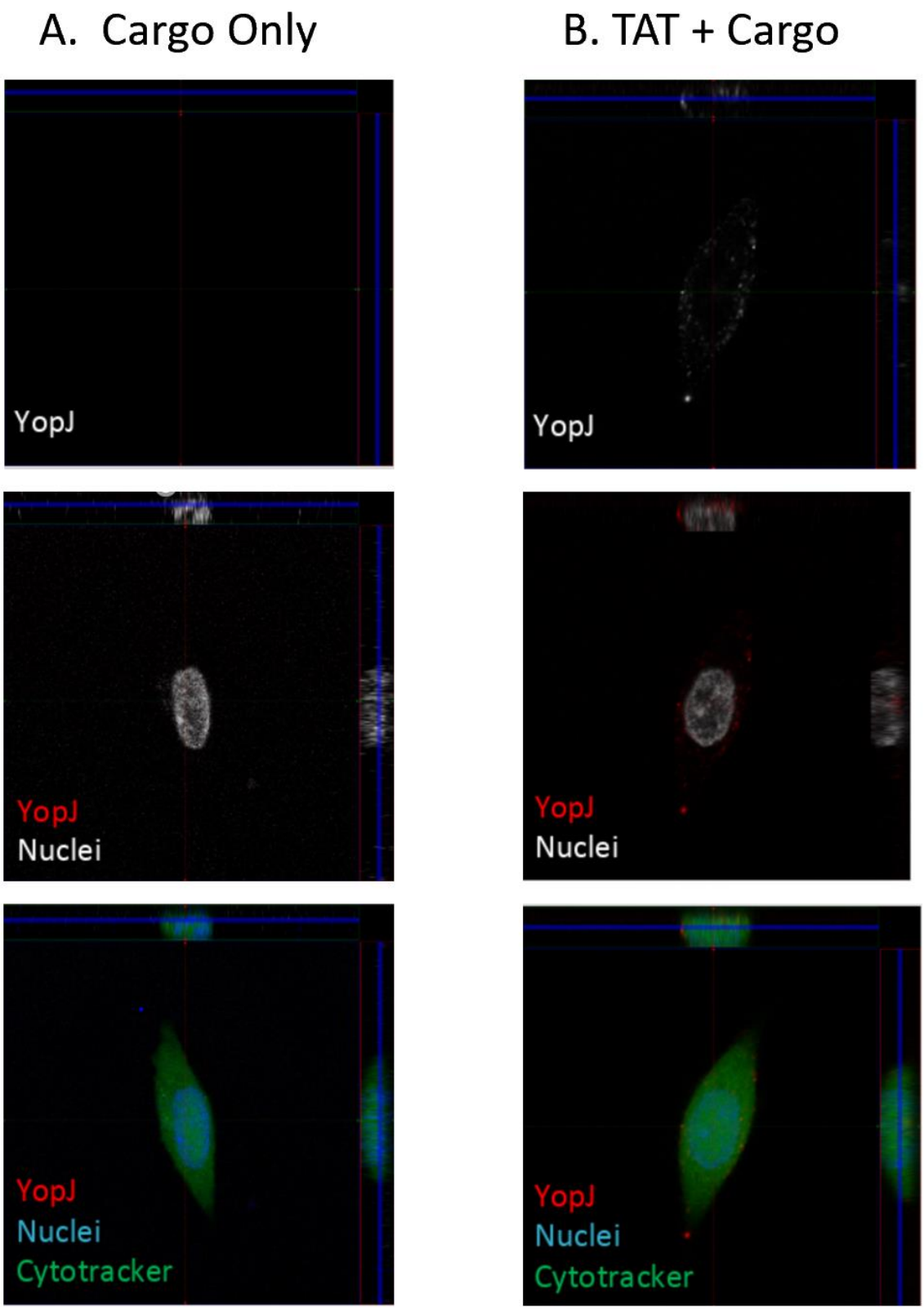
A. Cargo Only
B. TAT + Cargo
YopJ
YopJ
YopJ
Nuclei
YopJ
Nuclei
YopJ
Nuclei
Cytotracker
YopJ
Nuclei
Cytotracker

Figure 17: YopJ Uptake in SiHa Cells. YopJ was labeled with DyLight 550 red fluorescent tag. The cytoplasm was stained with 1mM CellTracker Green (Thermo Fisher Scientific). The nuclei were stained with NucBlue LiveReady Probes (Thermo Fisher Scientific). A. Cells that were treated with YopJ alone (no TAT-CaM). B. Cells that were treated with TAT-CaM-YopJ. These images suggest that YopJ is able to penetrate into the cell only when bound to TAT-CaM.

4. CELL DEATH ASSAYS

In order to quantify cell death resulting from TAT-CaM-Effector treatment, LDH assays were performed. LDH assays utilize lactase dehydrogenase (LDH) in the media as a measure of cell death. When cells die, membranes are compromised and LDH is allowed to leak into the media. The amount of LDH released per cell is remarkably uniform across a given cell type. Thus, it can be used to quantify what percentage of a cell population is dead. LDH in the media can be measured via a fluorometric assay that utilizes a fluorophore or via a colormetric assay that measures LDH reactivity with a substrate. We opted for the latter and chose the Pierce LDH cytotoxicity assay kit (Thermo Scientific). First, LDH catalyzes the conversion of lactate to pyruvate, resulting in NAD+ reduction to NADH. Then, diaphorase utilizes NADH to reduce tetrazolium salt (INT) into a red formazan product. The formation of this red formazan product creates a color change that can be detected on a microplate reader.

4.1 Preparation of Treatments and Controls:

TAT-CaM-Cargo:

Purified TAT-CaM and a purified bacterial effector were thawed in the presence of 200nM DTT and combined at a concentration of 10uM in 60uL NEB buffer (10mM Hepes, 150mM NaCl, 1mM $CaCl_2$, 10% Glycerol, 1mM DTT). The mixture was allowed to incubate on ice for 10 minutes to allow the TAT-CaM-Cargo complex to assemble. The complex was then diluted to 1uM via the addition of 550uL of sterile growth medium.

TAT-CaM Only and Cargo Only:

Purified protein was thawed in the presence of 200nM DTT, then serially diluted to 10uM in 60uL of NEB buffer (10mM Hepes, 150mM NaCl, 1mM $CaCl_2$, 10% Glycerol, 1mM DTT). The protein was then diluted to 1uM via the addition of 550uL of sterile growth medium.

4.2 Treatment of Cells

Cells were cultured in 96-well plates in Dulbecco's Modified Eagle Medium with 5% FBS. Experimental wells were treated with 1uM TAT-CaM-Cargo. Control wells were treated with 1μM of cargo only, TAT-CaM only or with nothing (no-treatment control). Each treatment was performed in triplicate.

4.3 Analysis of LDH Activity

At each time point, 50uL of media was removed from the cells and placed in a new 96-well plate to be tested for LDH content. 50uL of fresh media was then placed on the cells. To measure LDH levels in the media collected, 50uL of colormetric agent was added and allowed to react for 30 minutes in the dark at room temperature. Following this incubation, 100uL stop buffer was added to halt the reaction. Color change was measured on a microplate reader at 600nm.

4.4 Results and Discussion:

The initial cell death assay demonstrated a high level of cell death within the first hour post-treatment. The levels of cell death in cells treated with TAT-CaM-YopJ was not higher than that of the other treatments at the 6 and 24 hour time points due to the nature of the assay. In this assay, media is collected and tested after each time point and new media is added. The media that was collected from the wells containing TAT-CaM-YopJ was tested after the first hour and was shown to contain a large amount of LDH, indicating that a great deal of cell death occurred in the first hour. However, the LDH that had been produced was no longer in the well containing the cells and they failed to produce more by the 6 and 24 hour time periods. Thus, it was concluded that YopJ induces rapid cell death within the first hour post-treatment, but its effects are not dragged out over a long period of time.

Like in the intracellular delivery assays, data replication was a major issue with these cell death assays. Many times, no cell death was occurring at all. It is likely that this is the result of having to use a newer protein prep when the first one ran out. The first protein prep was very functional and Figure 19 shows the cell death data obtained from treating cells with it. However, none of the other preps produced the same results. So, it is likely that we had nonfunctional protein in the preps that came after the initial one.

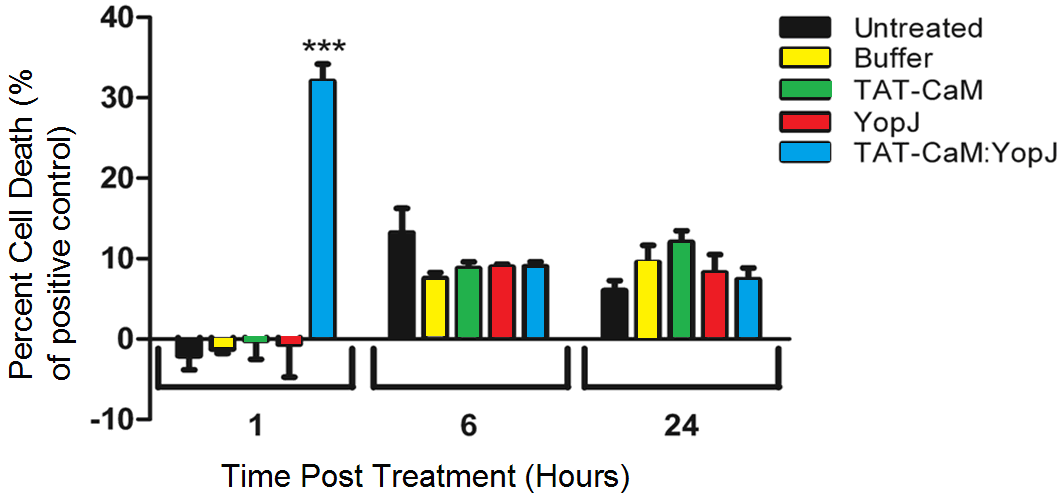

Figure 18: TAT-CaM-YopJ induced Cell Death in SiHa Cells. SiHa cells were subjected to 1uM treatments and resulting LDH leakage was monitored over a 24 hour period. TAT-CaM-YopJ induced significant levels of cell death within 1 hour post-treatment.

5. FUTURE DIRECTIONS

5.1 Reproducing Positive Uptake Results:

This study showed that the TAT-CaM system is capable of delivering bacterial effector proteins into mammalian cells without the need for bacterial infection and type-III secretion systems. Although many experiments resulted in the uptake of effectors without the TAT-CaM system, this can most likely be explained by cellular distress. One major cause of cell distress that was detected in this study was the presence of mycoplasma contamination in both cell lines. However, when the cells were healthy, the effectors were able to enter the cells only when bound to TAT-CaM. Thus, TAT-CaM seems to be an effective delivery mechanism for bacterial effector proteins. Future researchers must be sure to keep their cell lines free of mycoplasma and overall devoid of stress. It is likely that this would result in the reproducibility of the positive data obtained in this study.

5.2 Reproducing Positive Cell Death Assay Results:

This study also showed the ability of TAT-CaM-YopJ to induce rapid cell death in epithelial cancer cells within the first hour of treatment. However, reproducibility was once again an issue. The issues with reproducibility came after the original protein prep was exhausted. Thus, it is likely that a functional prep of YopJ would allow future researchers to achieve positive results more consistently.

5.3 Further Exploration of Effector Pathways:

In addition to reproducing the positive data obtained in this study, it would beneficial for a future researcher to pursue the identification of pathway interference by YopJ and VopA. While some MAP2Ks that are targeted by these effectors have been identified, there is not a comprehensive list of YopJ and VopA kinase interactions.

Additionally, the identification of the exact location of YopJ action in the apoptotic pathway has yet to be elucidated. It has been shown that YopJ stimulates the pathway somewhere between the death receptor and caspase-8. The details of this pathway could potentially be discovered through immunoblotting techniques.

5.4 Other Bacterial Effectors:

This study focused primarily on YopJ and included some experiments with VopA. However, there are hundreds of other bacterial effector proteins out there that could potentially be more effective than YopJ or VopA. Therefore, after establishing a consistent protocol and a healthy cell line to confirm the data obtained in this study, future researchers may benefit from expanding this study to other bacterial effectors in the hopes of identifying and even more effective effector with more potential as a cancer therapeutic.

5.5 Summation of Future Work Required:

This study produced data that would suggest that YopJ is able to be delivered into cancer cells via the TAT-CaM adaptor system and that this delivery is capable of inducing rapid cellular death. However, in order to say that this is the case with certainty, these experiments must be replicable. Thus, future research is required to confirm the results of this study.

Additionally, it is not only important to prove that this system can work, but to also be able to explain why it works. Therefore, future research into the pathways by which YopJ and VopA act would be highly beneficial.

YopJ and VopA are only two bacterial effectors out of hundreds. It may be that there are others which would work even more effectively. Therefore, this study could also be expanded to include many more bacterial effectors in order to determine the best effector for cancer therapeutics.

REFERENCES

[1] Jones, R. M., & Neish, A. S. (2011). Recognition of bacterial pathogens and mucosal immunity. Cellular Microbiology, 13(5), 670-676. doi:10.1111/j.1462-5822.2011.01579.x

[2] Jones, R. M., Luo, L., & Moberg, K. H. (2011). Aeromonas salmonicida-secreted protein AopP is a potent inducer of apoptosis in a mammalian and a Drosophila model. Cellular Microbiology,14(2), 274-285. doi:10.1111/j.1462-5822.2011.01717.x

[3] Jones, R. M., Wu, H., Wentworth, C., Luo, L., Collier-Hyams, L., & Neish, A. S. (2008). Salmonella AvrA Coordinates Suppression of Host Immune and Apoptotic Defenses via JNK Pathway Blockade. Cell Host & Microbe, 3(4), 233-244. doi:10.1016/j.chom.2008.02.016

[4] Ngwa, V. M., Axford, D. S., Healey, A. N., Nowak, S. J., Chrestensen, C. A., & McMurry, J. L. (2017). A versatile cell-penetrating peptide-adaptor system for efficient delivery of molecular cargos to subcellular destinations. Plos ONE, (5), doi:10.1371/journal.pone.0178648

[5] Salerno, J. C., Ngwa, V. M., Nowak, S. J., Chrestensen, C. A., Healey, A. N., & McMurry, J. L. (2016). Novel cell-penetrating peptide-adaptors effect intracellular delivery and endosomal escape of protein cargos. Journal Of Cell Science, 129(5), 893. doi:10.1242/jcs.182113

[6] Galluzzi, Lorenzo & Blomgren, Klas & Kroemer, Guido. (2009). Mitochondrial membrane permeabilization in neuronal injury. Nature reviews. Neuroscience. 10. 481-94. 10.1038/nrn2665.

[7] Ma, K., & Ma, W. (2016). Yopj family effectors promote bacterial infection through a unique acetyltransferase activity. Microbiology And Molecular Biology Reviews, 80(4), 1011-1027. doi:10.1128/MMBR.00032-16

[8] Scott, N. E., & Hartland, E. L. (2017). Review: Post-translational Mechanisms of Host Subversion by Bacterial Effectors. Trends In Molecular Medicine, 231088-1102. doi:10.1016/j.molmed.2017.10.003

[9] Rüter, C., & Schmidt, M. A. (2017). Opinion: Cell-Penetrating Bacterial Effector Proteins: Better Tools than Targets. Trends In Biotechnology, 35109-120. doi:10.1016/j.tibtech.2016.08.002

[10] Robinson, K. S., & Aw, R. (2016). Review: The Commonalities in Bacterial Effector Inhibition of Apoptosis. Trends In Microbiology, 24665-680. doi:10.1016/j.tim.2016.04.002

[11] Plotnikov, A., Zehorai, E., Procaccia, S., & Seger, R. (2011). The MAPK cascades: Signaling components, nuclear roles and mechanisms of nuclear translocation. *Biochimica Et Biophysica Acta (BBA) - Molecular Cell Research,1813*(9), 1619-1633. doi:10.1016/j.bbamcr.2010.12.012

[12] Cargnello, M., & Roux, P. P. (2011). Activation and Function of the MAPKs and Their Substrates, the MAPK-Activated Protein Kinases. *Microbiology and Molecular Biology Reviews : MMBR*, *75*(1), 50–83. http://doi.org/10.1128/MMBR.00031-10

[13] Ngwa, Verra M., "Novel Cell Penetrating Peptides Effect Endosomal Escape and Deliver Protein Cargos into Living Cells" (2016). *Master of Science in Chemical*

Sciences Theses. 10. https://digitalcommons.kennesaw.edu/mscs_etd/10

[14] Monack, D. M., Mecsas, J., Ghori, N., & Falkow, S. (1997). *Yersinia* signals macrophages to undergo apoptosis and YopJ is necessary for this cell death. *Proceedings of the National Academy of Sciences of the United States of America*, *94*(19), 10385–10390.

[15] Estrada, L. H., Padmore, T. J., & Champion, J. A. (2016). Bacterial Effector Nanoparticles as Breast Cancer Therapeutics. *Molecular Pharmaceutics,13*(3), 710-719. doi:10.1021/acs.molpharmaceut.5b00377

[16] Wall, D. M., & McCormick, B. A. (2014). Bacterial secreted effectors and caspase-3 interactions. *Cellular Microbiology*, *16*(12), 1746–1756. http://doi.org/10.1111/cmi.12368

[17] Zauberman, A., Cohen, S., Mamroud, E., Flashner, Y., Tidhar, A., Ber, R., … Velan, B. (2006). Interaction of *Yersinia pestis* with Macrophages: Limitations in YopJ-Dependent Apoptosis . *Infection and Immunity*, *74*(6), 3239–3250. http://doi.org/10.1128/IAI.00097-06

[18] Galán, J. E. (1999). Type III Secretion Machines: Bacterial Devices for Protein Delivery into Host Cells. *Science,284*(5418), 1322-1328. doi:10.1126/science.284.5418.1322

[19] Hensel, M., Shea, J. E., Waterman, S. R., Mundy, R., Nikolaus, T., Banks, G., . . . Holden, D. W. (1998). Genes encoding putative effector proteins of the type III secretion system ofSalmonellapathogenicity island 2 are required for bacterial virulence and proliferation in macrophages. *Molecular Microbiology,30*(1), 163-174.

doi:10.1046/j.1365-2958.1998.01047.x

[20] Orth, K. (2000). Disruption of Signaling by Yersinia Effector YopJ, a Ubiquitin-Like Protein Protease. *Science,290*(5496), 1594-1597. doi:10.1126/science.290.5496.1594

[21] Mattoo, S., Lee, Y. M., & Dixon, J. E. (2007). Interactions of bacterial effector proteins with host proteins. *Current Opinion in Immunology,19*(4), 392-401. doi:10.1016/j.coi.2007.06.005

[22] Klumpp, D. J., Rycyk, M. T., Chen, M. C., Thumbikat, P., Sengupta, S., & Schaeffer, A. J. (2006). Uropathogenic Escherichia coli Induces Extrinsic and Intrinsic Cascades To Initiate Urothelial Apoptosis. *Infection and Immunity,74*(9), 5106-5113. doi:10.1128/iai.00376-06

[23] Mukherjee, S. (2006). Yersinia YopJ Acetylates and Inhibits Kinase Activation by Blocking Phosphorylation. *Science,312*(5777), 1211-1214. doi:10.1126/science.1126867

[24] Galán, J. E. "Type III Secretion Machines: Bacterial Devices for Protein Delivery into Host Cells." *Science*, vol. 284, no. 5418, 1999, pp. 1322–1328., doi:10.1126/science.284.5418.1322.

[25] Tsai, Chi-Lin, et al. "The Salmonella Type III Secretion System Virulence Effector Forms a New Hexameric Chaperone Assembly for Export of Effector/Chaperone Complexes." *Journal of Bacteriology*, vol. 197, no. 4, Aug. 2014, pp. 672–675., doi:10.1128/jb.02524-14.

[26] Abby, Sophie S., and Eduardo P. C. Rocha. "The Non-Flagellar Type III Secretion System Evolved from the Bacterial Flagellum and Diversified into Host-Cell Adapted Systems." *PLoS Genetics*, vol. 8, no. 9, 2012, doi:10.1371/journal.pgen.1002983.

[27] Robert, J. R. (2012) ERK1/2 MAP kinases: structure, function, and regulation. *Pharmacol. Res.* **66**, 105–143

[28] Editors. “Apoptosis: Definition, Pathway, Examples and Quiz.” *Biology Dictionary*, Biology Dictionary, 6 June 2017, biologydictionary.net/apoptosis/.

[29] Allolio, Christoph, et al. “Arginine-Rich Cell-Penetrating Peptides Induce Membrane Multilamellarity and Subsequently Enter via Formation of a Fusion Pore.” *Proceedings of the National Academy of Sciences*, vol. 115, no. 47, 2018, pp. 11923–11928., doi:10.1073/pnas.1811520115.

[30] Raucher, Drazen, and Jung Su Ryu. “Cell-Penetrating Peptides: Strategies for Anticancer Treatment.” *Trends in Molecular Medicine*, vol. 21, no. 9, 2015, pp. 560–570., doi:10.1016/j.molmed.2015.06.005.

[31] Popa, Crina M., et al. “Modification of Bacterial Effector Proteins Inside Eukaryotic Host Cells.” *Frontiers in Cellular and Infection Microbiology*, vol. 6, 2016, doi:10.3389/fcimb.2016.00073.

[32] Rüter, Christian, and Philip R. Hardwidge. “‘Drugs from Bugs’: Bacterial Effector Proteins as Promising Biological (Immune-) Therapeutics.” *FEMS Microbiology Letters*, vol. 351, no. 2, 2013, pp. 126–132., doi:10.1111/1574-6968.12333.

[33] Dean, Paul. “Functional Domains and Motifs of Bacterial Type III Effector Proteins and Their Roles in Infection.” *FEMS Microbiology Reviews*, vol. 35, no. 6, 2011, pp. 1100–1125., doi:10.1111/j.1574-6976.2011.00271.x.

[34] Galán, Jorge E. “Common Themes in the Design and Function of Bacterial Effectors.” *Cell Host & Microbe*, vol. 5, no. 6, 2009, pp. 571–579., doi:10.1016/j.chom.2009.04.008.

[35] Grabowski, Benjamin, et al. “Immunomodulatory Yersinia Outer Proteins (Yops)–Useful Tools for Bacteria and Humans Alike.” *Virulence*, vol. 8, no. 7, 2017, pp. 1124–1147., doi:10.1080/21505594.2017.1303588.

[36] Kendall, Melissa M. “Extra! Extracellular Effector Delivery into Host Cells via the Type 3 Secretion System.” *MBio*, vol. 8, no. 3, 2017, doi:10.1128/mbio.00594-17.

[37] Verma, Ayush, et al. “Erratum: Surface-Structure-Regulated Cell-Membrane Penetration by Monolayer-Protected Nanoparticles.” *Nature Materials*, vol. 12, no. 4, 2013, pp. 376–376., doi:10.1038/nmat3593.

[38] Allbritton, Nancy. “Faculty of 1000 Evaluation for Cell-Penetrating Peptides. A Reevaluation of the Mechanism of Cellular Uptake.” *F1000 - Post-Publication Peer Review of the Biomedical Literature*, 2002, doi:10.3410/f.1011095.177314.

[39] Morris, M, et al. “A Peptide Carrier for the Delivery of Biologically Active Proteins into Mammalian CellsApplication to the Delivery of Antibodies and Therapeutic Proteins.” *Cell Biology*, 2006, pp. 13–18., doi:10.1016/b978-012164730-8/50187-8.

[40] Rappuoli, Rino. “Faculty of 1000 Evaluation for Acetylation of MEK2 and I Kappa B Kinase (IKK) Activation Loop Residues by YopJ Inhibits Signaling.” *F1000 - Post-Publication Peer Review of the Biomedical Literature*, 2006, doi:10.3410/f.1052969.504920.

[41] Schesser, Kurt, et al. “The YopJ Locus Is Required for Yersinia-Mediated Inhibition of NF-KappaB Activation and Cytokine Expression: YopJ Contains a Eukaryotic SH2-like Domain That Is Essential for Its Repressive Activity.” *Molecular Microbiology*, vol. 28, no. 6, 1998, pp. 1067–1079., doi:10.1046/j.1365-2958.1998.00851.x.

[42] Orth, K. “Function of the Yersinia Effector YopJ.” *Current Opinion in Microbiology*, vol. 5, no. 1, 2002, pp. 38–43., doi:10.1016/s1369-5274(02)00283-7.

[43] Kale, V.p. “Differential Activation of MAPK Signaling Pathways by TGF-β1 Forms the Molecular Mechanism Behind Its Dose-Dependent Bidirectional Effects on Hematopoiesis.” *Stem Cells and Development*, vol. 13, no. 1, 2004, pp. 27–38., doi:10.1089/154732804773099236.

[44] Krismer, Konstantin, et al. “Scansite.” *Scansite 4.0*, scansite4.mit.edu/4.0/#home.

[45] “A Protein Secondary Structure Prediction Server.” *JPred: A Protein Secondary Structure Prediction Server*, www.compbio.dundee.ac.uk/jpred4.

[46] Elmore, Susan. “Apoptosis: a Review of Programmed Cell Death.” *Toxicologic Pathology*, U.S. National Library of Medicine, 2007, www.ncbi.nlm.nih.gov/pubmed/17562483.

[47] Thompson, CB. “Apoptosis in the Pathogenesis and Treatment of Disease.” *Science*, American Association for the Advancement of Science, 10 Mar. 1995, science.sciencemag.org/content/267/5203/1456.

[48] Wei, M C, et al. “Proapoptotic BAX and BAK: a Requisite Gateway to Mitochondrial Dysfunction and Death.” *Science (New York, N.Y.)*, U.S. National Library of Medicine, 27 Apr. 2001, www.ncbi.nlm.nih.gov/pmc/articles/PMC3049805/.

[49] *Bid Truncation, Bid/Bax Targeting to the Mitochondria, and* ...www.researchgate.net/profile/Dirk_Roos/publication/8551855_Bid_Truncation_BidBax_Targeting_to_the_Mitochondria_and_Caspase_Activation_Associated_with_Neutrophil_Apoptosis_Are_Inhibited_by_Granulocyte_Colony-

Stimulating_Factor/links/54e742960cf277664ff8ae22.pdf?inViewer=true&pdfJsDownload=true&disableCoverPage=true&origin=publication_detail.

[50] "PLASMID DNA PREPARATION." *GENEWIZ*, www.genewiz.com/Public/Services/Plasmid-DNA-Prep/Standard?sc_camp=6FABC3F1DE834A56AAB57CA17A06331A&ads_adid=59092998468&ads_cmpid=1027908458&ads_creative=301960060529&ads_matchtype=b&ads_network=g&ads_targetid=kwd-541688600543&ttv=2&utm_campaign=adwords&utm_medium=ppc&utm_source=adwords&utm_term=plasmid prep service&gclid=CjwKCAjwza_mBRBTEiwASDWVvhImXK8PQv-xCIEmil8oipVt3DT9kds065CpDLJRG8cj1-R9MmfPChoC6F8QAvD_BwE.

[51] "Precision Plus Protein™ Dual Color Standards, 500 Ml #1610374." *Bio*, www.bio-rad.com/en-us/sku/1610374-precision-plus-protein-dual-color-standards-500-ul?ID=1610374.

[52] Ryan KJ, Ray CG (editors) (2004). Sherris Medical Microbiology (4th ed.). McGraw Hill. pp. 409–12. ISBN 978-0-8385-8529-0.